Article

Cell Reports

The Transcription Factor MAZR/PATZ1 Regulates the Development of FOXP3^{+} Regulatory T Cells

Graphical Abstract

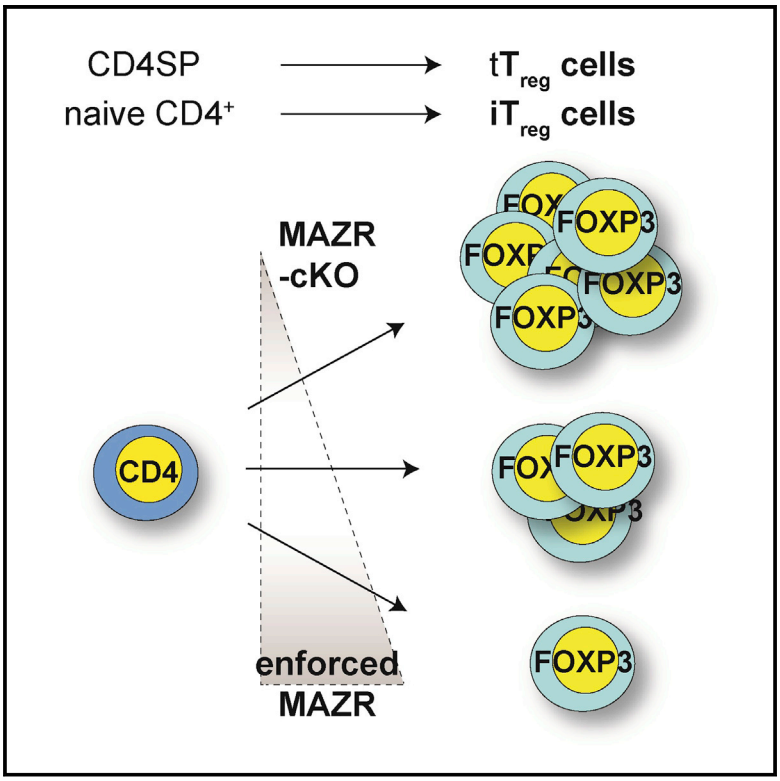

Authors

Liisa Andersen, Alexandra Franziska Gülich, Marlis Alteneder, ..., Riitta Lahesmaa, Shinya Sakaguchi, Wilfried Ellmeier

Correspondence

wilfried.ellmeier@meduniwien.ac.at

In Brief

FOXP3^{+} T_{reg} cells are essential for maintaining tolerance and immune homeostasis. Andersen et al. reveal that MAZR is an important factor in regulating the delicate balance of T_{reg} cell generation and report that MAZR expression levels play a key role in controlling T_{reg} cell development and differentiation.

Highlights

- FOXP3^{+} T_{reg} cell generation is enhanced upon deletion of MAZR
- Enforced expression of MAZR impairs T_{reg} cell generation
- MAZR expression levels are downregulated during T_{reg} cell differentiation
- T cell-specific deletion of MAZR reduces clinical score of DSS-induced colitis

Andersen et al., 2019, Cell Reports *29*, 4447–4459
December 24, 2019
https://doi.org/10.1016/j.celrep.2019.11.089

CellPress

Cell Reports
Article

The Transcription Factor MAZR/PATZ1 Regulates the Development of FOXP3$^+$ Regulatory T Cells

Liisa Andersen,[1] Alexandra Franziska Gülich,[1] Marlis Alteneder,[1] Teresa Preglej,[1] Maria Jonah Orola,[1,9] Narendra Dhele,[1] Valentina Stolz,[1] Alexandra Schebesta,[1] Patricia Hamminger,[1] Anastasiya Hladik,[2] Stefan Floess,[3] Thomas Krausgruber,[4] Thomas Faux,[5] Syed Bilal Ahmad Andrabi,[7] Jochen Huehn,[3] Sylvia Knapp,[2,4] Tim Sparwasser,[8] Christoph Bock,[4,6] Asta Laiho,[5] Laura L. Elo,[5] Omid Rasool,[7] Riitta Lahesmaa,[7] Shinya Sakaguchi,[1] and Wilfried Ellmeier[1,10,*]

[1]Division of Immunobiology, Institute of Immunology, Center for Pathophysiology, Infectiology and Immunology, Medical University of Vienna, Vienna, Austria
[2]Laboratory of Infection Biology, Department of Medicine I, Medical University of Vienna, Vienna, Austria
[3]Experimental Immunology, Helmholtz Centre for Infection Research, Braunschweig, Germany
[4]CeMM Research Center for Molecular Medicine of the Austrian Academy of Sciences, Vienna, Austria
[5]Medical Bioinformatics Centre, Turku Bioscience Centre, University of Turku and Åbo Akademi University, Turku, Finland
[6]Department of Laboratory Medicine, Medical University of Vienna, Vienna, Austria
[7]Molecular Systems Immunology, Turku Bioscience Centre, University of Turku and Åbo Akademi University, Turku, Finland
[8]Department of Medical Microbiology and Hygiene, Medical Center of the Johannes Gutenberg-University of Mainz, Mainz, Germany
[9]Present address: Institute of Specific Prophylaxis and Tropical Medicine, Center for Pathophysiology, Infectiology and Immunology, Medical University of Vienna, Vienna, Austria
[10]Lead Contact
*Correspondence: wilfried.ellmeier@meduniwien.ac.at
https://doi.org/10.1016/j.celrep.2019.11.089

SUMMARY

Forkhead box protein P3$^+$ (FOXP3$^+$) regulatory T cells (T_{reg} cells) play a key role in maintaining tolerance and immune homeostasis. Here, we report that a T cell-specific deletion of the transcription factor MAZR (also known as PATZ1) leads to an increased frequency of T_{reg} cells, while enforced MAZR expression impairs T_{reg} cell differentiation. Further, MAZR expression levels are progressively downregulated during thymic T_{reg} cell development and during *in-vitro*-induced human T_{reg} cell differentiation, suggesting that MAZR protein levels are critical for controlling T_{reg} cell development. However, MAZR-deficient T_{reg} cells show only minor transcriptional changes *ex vivo*, indicating that MAZR is not essential for establishing the transcriptional program of peripheral T_{reg} cells. Finally, the loss of MAZR reduces the clinical score in dextran-sodium sulfate (DSS)-induced colitis, suggesting that MAZR activity in T cells controls the extent of intestinal inflammation. Together, these data indicate that MAZR is part of a T_{reg} cell-intrinsic transcriptional network that modulates T_{reg} cell development.

INTRODUCTION

Forkhead box protein P3$^+$ (FOXP3$^+$) regulatory T cells (T_{reg} cells) are essential for maintaining T cell tolerance as well as tissue integrity throughout the lifespan of an organism. The dysregulation of T_{reg} cell functions is linked to autoimmunity; thus, their development and effector activity have to be tightly regulated (Josefowicz et al., 2012; Kitagawa and Sakaguchi, 2017; Li and Zheng, 2015). The majority of T_{reg} cells develop in the thymus (thymic-derived T_{reg} cells [tT_{reg} cells]) from CD25$^+$FOXP3$^-$CD4 single-positive (SP) T_{reg} precursor cells (Burchill et al., 2008; Lio and Hsieh, 2008). In addition, a fraction of T_{reg} cells are also induced upon activation of peripheral naive CD4$^+$ T cells (Curotto de Lafaille and Lafaille, 2009). FOXP3, a member of the FOXP transcription factor family, is essential and sufficient for the induction of T_{reg} cells and their suppressive activity (Fontenot et al., 2003; Hori et al., 2003; Khattri et al., 2003). Moreover, FOXP3 is required for maintaining the suppressive activity of T_{reg} cells (Williams and Rudensky, 2007). Although the transcriptional networks that regulate the induction and maintenance of *Foxp3* expression as well as the major *cis*-regulatory elements driving *Foxp3* expression have been identified (Huehn and Beyer, 2015; van der Veeken et al., 2013), the understanding of its transcriptional fine-tuning is still incomplete.

We previously identified the BTB (Broad-Complex, Tramtrack, and Bric a brac) domain-containing transcription factor MAZR (encoded by the *Patz1* gene) as an important factor during T cell development. MAZR is a negative regulator of CD8 expression during the double-negative (DN) to double-positive (DP) transition that prevents premature expression of CD8 in DN thymocytes, in part also by epigenetic mechanisms (Bilic et al., 2006). Moreover, by generating MAZR-deficient mice, we revealed that MAZR is part of the transcription factor network that controls CD4/CD8 cell-fate choice by repressing ThPOK expression (encoded by the *Zbtb7b* gene) in major histocompatibility complex (MHC)-class-I-signaled DP cells, thus preventing the redirection of developing CD8SP cells into the CD4 lineage (Sakaguchi et al., 2010). Subsequent studies using mice with a T cell-specific deletion of *Mazr* demonstrated that MAZR represses *Zbtb7b* in synergy with Runx1 in preselection DP cells and with Runx3 in CD8$^+$ T cells (Sakaguchi et al., 2015). Together, these studies show that MAZR is an important regulator of CD8 lineage differentiation. Whether

MAZR is important for the control of CD4 lineage development and/or the regulation of $CD4^+$ effector T cells has not yet been investigated.

In the present study, we investigated the role of MAZR in the generation of $FOXP3^+$ T_{reg} cells. We observed that a T cell-specific loss of MAZR led to an increased number of $FOXP3^+$ T_{reg} cells under homeostatic conditions *in vivo*. The generation of mixed bone marrow (BM) chimeric mice further revealed that a T_{reg} cell-intrinsic alteration led to the enhanced generation of T_{reg} cells. Moreover, MAZR-deficient naive $CD4^+$ T cells also showed an enhanced differentiation into inducible T_{reg} cells *in vitro*, indicating that MAZR deficiency promotes the generation of T_{reg} cells both *in vivo* and *in vitro*. In contrast, retroviral-mediated enforced expression of MAZR impaired T_{reg} cell development as well as *in vitro* T_{reg} cell (iT_{reg} cell) differentiation, suggesting a critical role not only for MAZR activity, but also for MAZR expression levels during the generation of T_{reg} cells. Correspondingly, MAZR expression levels were progressively downregulated during murine T_{reg} cell development in the thymus as well as during murine and human iT_{reg} cell differentiation *in vitro*. RNA sequencing (RNA-seq) of peripheral MAZR-conditional knockout (cKO) T_{reg} cells revealed a low number of dysregulated genes, indicating that MAZR is not essential for establishing the T_{reg} cell transcriptome. Finally, MAZR-cKO mice displayed a reduced clinical score in a dextran-sodium sulfate (DSS)-induced colitis model, suggesting a protective role for the activity of MAZR in T cells against DSS-induced colitis. Together, these data strongly suggest that MAZR modulates the generation of $FOXP3^+$ T_{reg} cells.

RESULTS

Loss of MAZR Leads to an Increase in $FOXP3^+$ T_{reg} Cells

We recently generated mice with a T cell-specific deletion of MAZR using *Cd4*-Cre (Sakaguchi et al., 2015). During the analysis of $Mazr^{F/F}$*Cd4*-Cre mice (designated as MAZR-cKO throughout the manuscript), we observed that the percentage and number of T_{reg} cells increased in MAZR-cKO mice in comparison to $Mazr^{F/F}$ (wild-type [WT]) controls (Figures 1A and 1B), while the FOXP3 expression level (i.e., mean fluorescence intensity [MFI]) within the T_{reg} cell subset was unchanged (Figure 1C). An increase in $FOXP3^+$ T_{reg} cells was already evident in 5-day-old MAZR-cKO neonates, indicating that the alterations in T_{reg} cell generation observed in adult mice are already present shortly after birth (Figures 1D and 1E). To test whether the increase in $FOXP3^+$ T_{reg} cells correlated with enhanced *Foxp3* gene expression, we crossed WT and MAZR-cKO mice on the DEREG (depletion of regulatory T cells) *Foxp3*-EGFP reporter, in which EGFP expression is driven by *Fopx3* regulatory elements (Lahl et al., 2007). This revealed that $EGFP^+$ T_{reg} cells were also increased in the absence of MAZR (Figure 1F), suggesting that the phenotype observed was due to an induction of *Foxp3* mRNA gene expression in a fraction of cells that otherwise would not express *Foxp3* during T_{reg} cell generation. Of note, we also observed an increase in $FOXP3^+$ $CD8^+$ T cells in MAZR-cKO mice (Figure 1G), indicating that MAZR controls the extent of FOXP3 expression both in $CD4^+$ and in $CD8^+$ T cells. To test whether this effect was T_{reg} cell intrinsic, we generated either WT ($CD45.1^+$) and $Mazr^{+/+}$*Lck*-Cre ($CD45.2^+$) or WT ($CD45.1^+$) and $Mazr^{F/F}$*Lck*-Cre ($CD45.2^+$) mixed BM chimeric mice. The percentage of $FOXP3^+$ $CD4^+$ T cells was significantly increased within the $CD45.2^+$ fraction in chimeric mice receiving MAZR-deficient BM, compared to the corresponding $CD45.2^+$ fraction in mice receiving MAZR-sufficient BM (Figures S1A–S1C). This demonstrates that the increase in $FOXP3^+$ T cells in the absence of MAZR is due to a T_{reg} cell-intrinsic effect.

To study whether a loss of MAZR also changes the *in vitro* generation of iT_{reg} cells, WT and MAZR-cKO naive $CD4^+$ T cells were differentiated into iT_{reg} cells using transforming growth factor β (TGF-β). Consistent with tT_{reg} cell development, the loss of MAZR enhanced the generation of $FOXP3^+$ T cells in iT_{reg} cell cultures as well (Figures 2A and 2B). Similar to tT_{reg} cell development, *Foxp3* gene expression was induced in a greater fraction in MAZR-deficient iT_{reg} cell cultures, since we also observed an increase in EGFP expression from the DEREG reporter allele upon differentiation of MAZR-cKO,DEREG $CD4^+$ T cells in comparison to WT,DEREG $CD4^+$ T cells (Figure 2C). WT and MAZR-cKO $CD4^+$ T cells displayed a similar proliferation as well as survival rate during iT_{reg} cell differentiation (Figures 2D and 2E), suggesting that the observed effect is due to an enhanced *in vitro* differentiation potential of naive MAZR-deficient $CD4^+$ T cells toward T_{reg} cells. *Foxp3* gene expression is regulated by at least three conserved noncoding sequences (CNS1, CNS2, and CNS3) (Zheng et al., 2010). Among those, CNS1 is TGF-β sensitive and critical for the generation of iT_{reg} cells (Schlenner et al., 2012; Tone et al., 2008; Zheng et al., 2010). CNS1 also transactivates reporter gene expression in $CD4^+$ T cells under iT_{reg} cell-inducing conditions in transient luciferase assays (Polansky et al., 2010). In agreement with these published data (Polansky et al., 2010), we observed a basal activity of the *Foxp3* promoter as well as an activity of CNS1 in WT iT_{reg} cells; however, the activity of these *cis*-elements was not significantly changed between WT and MAZR-cKO iT_{reg} cells (Figure 2F). Thus, MAZR negatively regulates the generation of tT_{reg} cells as well as iT_{reg} cells but does not alter the activity of CNS1.

It has been reported that iT_{reg} cells downregulate FOPX3 expression upon restimulation in the absence of TGF-β, while FOXP3 expression is stable in *ex vivo* isolated and reactivated T_{reg} cells (Floess et al., 2007). To test whether MAZR regulates the maintenance of FOXP3 expression in iT_{reg} cells, we sorted WT and MAZR-cKO iT_{reg} cells (using DEREG-GFP expression as a surrogate marker for FOXP3) and restimulated the cells with anti-CD3/anti-CD28 in the absence of TGF-β for 4 days. In agreement with the previous study (Floess et al., 2007), we observed that WT $FOXP3^+$ iT_{reg} cells progressively lost FOXP3 expression (Figure 2G). Although FOXP3 expression was also downmodulated in MAZR-cKO iT_{reg} cells on day 4, the percentage of MAZR-cKO iT_{reg} cells that expressed FOXP3 on day 2 was higher compared to WT iT_{reg} cells (Figure 2G). These data suggest that MAZR regulates the initial stability of *Foxp3* expression after reactivation in the absence of TGF-β. Of note, *ex vivo* isolated and activated WT and MAZR-cKO T_{reg} cells stably maintained FOXP3 expression to a similar degree (data not shown).

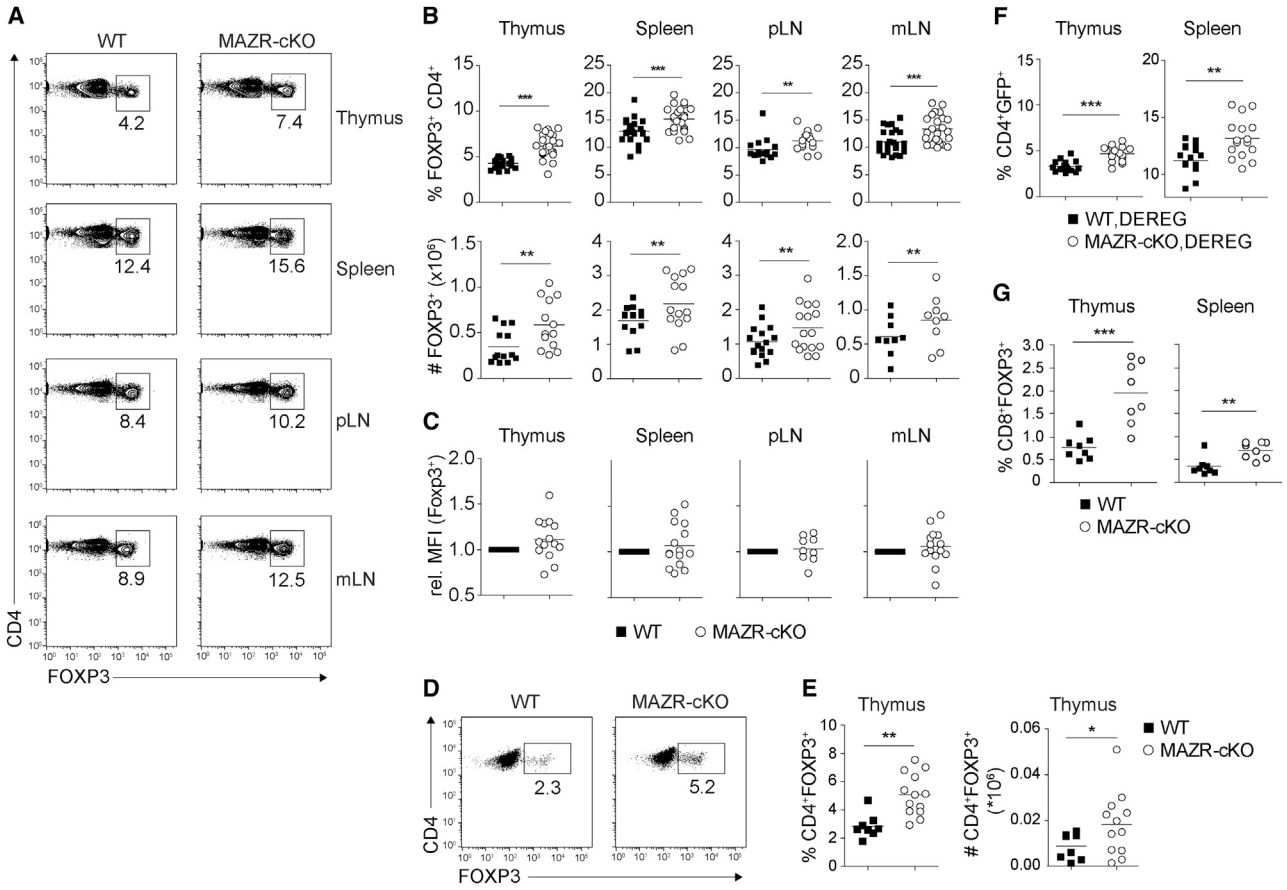

Figure 1. A T Cell-Specific Deletion of *Mazr* Leads to an Increase of FOXP3$^+$ tT$_{reg}$ Cells

(A) Flow cytometry analysis showing CD4 and intracellular FOXP3 expression in WT and MAZR-cKO TCRβ$^+$ cells isolated from thymus, spleen, peripheral LNs (pLNs), and mesenteric LNs (mLNs).

(B) Diagrams show the percentage (%; upper panel) and the total number (#; lower panel) of WT and MAZR-cKO FOXP3$^+$CD4$^+$ T cells.

(C) Diagrams indicate the mean fluorescence intensity (MFI) of FOXP3 expression in WT and MAZR-cKO CD4$^+$ T cells (WT MFI levels were set as 1, and relative MFI levels in MAZR-cKO CD4$^+$ T cells are shown).

(D) Flow cytometry analysis shows CD4 and intracellular FOXP3 expression in WT and MAZR-cKO TCRβ$^+$ cells isolated from thymi of 5-day-old neonates.

(E) Diagrams show the percentage (%; left panel) and the total number (#; right panel) of WT and MAZR-cKO FOXP3$^+$CD4$^+$ thymocytes from 5-day-old neonates.

(F) Diagrams show the percentage of EGFP$^+$ (i.e., FOXP3$^+$) cells within DEREG,WT and DEREG,MAZR-cKO CD4SP thymocytes and CD4$^+$TCRβ$^+$ splenocytes.

(G) Diagrams show the percentage of FOXP3$^+$ T$_{reg}$ cells within CD8SP thymocytes and CD8$^+$ splenocytes from WT and MAZR-cKO mice.

(A and D) Numbers indicate the percentage of cells in the respective gate. (B, C, and E–G) Each symbol indicates one mouse. Horizontal bars indicate the mean. *p < 0.05, **p < 0.01, and ***p < 0.001 (unpaired two-tailed Student's t test). Data are representative (A and D) or show the summary (B, C, and E–G) of at least 9 (A and B), 8 (C–E and G), or 16 (F) mice that were analyzed in at least 9 (A and B), 8 (C, F, and G) and 2 (D and E) independent experiments.

Foxp3 gene expression is also regulated at an epigenetic level (Huehn and Beyer, 2015). CNS2 constitutes a regulatory region that is methylated in thymocytes and selectively demethylated in *ex vivo* isolated FOXP3$^+$ T$_{reg}$ cells (T$_{reg}$ cell-specific -demethylated region [TSDR]) (Floess et al., 2007). CNS2 demethylation is required for the generation of stable T$_{reg}$ cells (Toker et al., 2013). Since MAZR is part of the transcriptional network that controls the *Cd8* gene locus at an epigenetic level (Bilic et al., 2006; Sakaguchi et al., 2010), we tested whether a loss of MAZR leads to changes in the methylation state of CNS2 (e.g., CD4$^+$CD25$^+$ precursor T$_{reg}$ cells show reduced methylation and thus are prone to more rapidly induce *Foxp3* expression). However, bisulphite sequencing of CD4SP CD25$^+$EGFP$^-$ precursor T$_{reg}$ cells isolated from WT,DEREG and MAZR-cKO,DEREG mice did not reveal any differences in the methylation status of the TSDR in the absence of MAZR (Figures S2A and S2B). There was also no difference between WT and MAZR-cKO mice in the degree of partial demethylation of the TSDR within CD4SP CD25$^+$EGFP$^+$ mature T$_{reg}$ cells (Figures S2A and S2B) (Toker et al., 2013). Thus, our data indicate that a loss of MAZR promotes the induction of *Foxp3* expression in CD4$^+$CD25$^+$ thymocytes, though the deletion of MAZR does not lead to changes in the TSDR methylation status in the CD4$^+$CD25$^+$ precursor T$_{reg}$ cell population. Of note, there was also no difference in the activity of CNS2 in transient luciferase assays between WT and MAZR-cKO iT$_{reg}$ cells (Figure S2C).

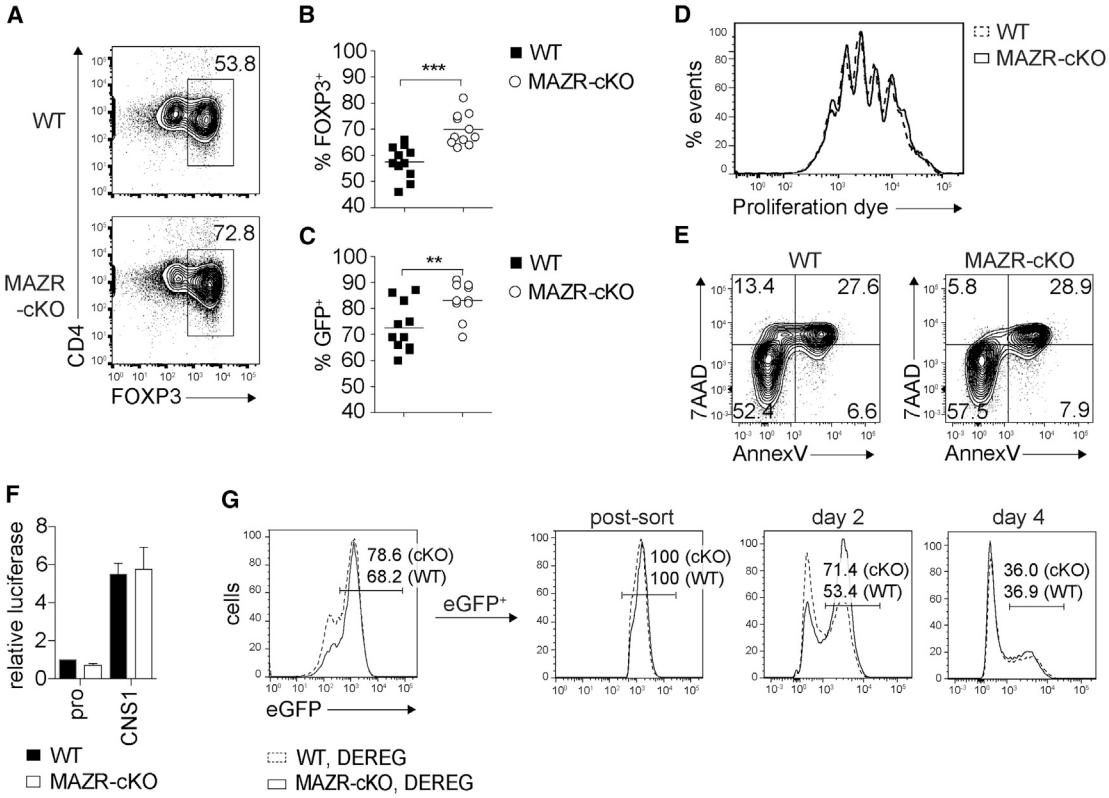

Figure 2. Loss of MAZR Enhances Differentiation of *In-Vitro*-Induced Regulatory T Cells

(A) Flow cytometry analysis shows CD4 and FOXP3 expression in naive WT and MAZR-cKO $CD4^+$ T cells activated with anti-CD3 and anti-CD28 for 3 days in the presence of TGF-β.

(B) Diagram shows the percentage of FOXP3-expressing cells of all experiments performed as in (A).

(C) Summary shows the percentage of $EGFP^+$ cells in WT,DEREG and MAZR-cKO,DEREG iT_{reg} cell cultures.

(D) Flow cytometry analysis depicts cell divisions of proliferation-dye-labeled WT and MAZR-cKO naive $CD4^+$ T cells activated with anti-CD3 and anti-CD28 for 3 days in the presence of TGF-β.

(E) 7AAD/AnnexinV staining of WT and MAZR cKO naive $CD4^+$ T cells activated as described in (A).

(F) Magnetic-activated cell sorting (MACS)-purified splenic $CD4^+$ T cells were stimulated with anti-CD3 and anti-CD28 in the presence of TGF-β for 72 h and subsequently electroporated with the indicated pGL4-based luciferase constructs. Diagram shows the summary of *Foxp3* promoter and CNS1 activity. Luciferase counts were normalized for transfection efficiency, and values relative to WT *Foxp3* promoter activity are shown. pro, *Foxp3*-promoter-luciferase; CNS1, CNS1-*Foxp3*-promoter-luciferase.

(G) WT,DEREG and MAZR-cKO,DEREG iT_{reg} cells were generated (using anti-CD3/anti-CD28 + TGF-β). $FOXP3^+$ cells (i.e., $EGFP^+$ cells) were sorted on day 3 and restimulated with anti-CD3/anti-CD28 in the absence of TGF-β. EGFP expression was assessed at day 2 and day 4 after restimulation.

(A, E, and G) Numbers indicate the percentage of cells in the respective quadrants or gates. (B and C) Each symbol indicates one mouse. Horizontal bars indicate the mean. $^{**}p < 0.01$ and $^{***}p < 0.001$ (unpaired two-tailed Student's t test). Data are representative (A, D, E, and G) or show the summary (B, C, and F) of at least 9 (A and B), 4 (C), 5 (D), or 2 (E and G) independent experiments. Data in (F) show summary of 4 independent biological batches performed in 2 independent experiments.

MAZR Is Progressively Downmodulated during Mouse and Human iT_{reg} Cell Differentiation

It has been shown that T_{reg} cells develop from a CD4SP $CD25^+$ progenitor cell population that upregulates FOXP3 (Burchill et al., 2008; Lio and Hsieh, 2008), although FOXP3 can also be induced before CD25 expression (Tai et al., 2013). In MAZR-cKO mice, both the $CD25^+FOXP3^+$ and the $CD25^-FOXP3^+$ populations were increased but not the $CD25^+FOXP3^-$ population (Figure 3A). Intracellular staining of the MAZR protein within the $TCR\beta^{hi}$CD4SP subset revealed lower MAZR expression levels in $CD4^+CD25^-FOXP3^+$ and $CD4^+CD25^+FOXP3^+$ T_{reg} cells in comparison to $CD4^+CD25^-$ and $CD4^+CD25^+$ subsets (Figures 3B and 3C). To test whether a similar downmodulation is also observed during iT_{reg} cell differentiation, we determined MAZR expression levels and FOXP3 expression during T cell activation under T helper 0 (Th0) and iT_{reg} cell culture conditions (anti-CD3/anti-CD28 ± TGF-β). MAZR expression was induced upon the activation of naive $CD4^+$ T cells, and MAZR levels remained high under Th0 conditions (Figure 3D). In contrast, we observed a less-pronounced induction of MAZR in the presence of TGF-β compared to Th0 conditions, and MAZR levels progressively decreased, while the percentage of $FOXP3^+$ cells steadily increased under iT_{reg} conditions (Figure 3D). Of note, in the absence of MAZR, the percentage of $FOXP3^+$ cells was already higher 24 h after activation compared to the WT iT_{reg} cultures (Figure S2D). However, there was no difference in MAZR protein

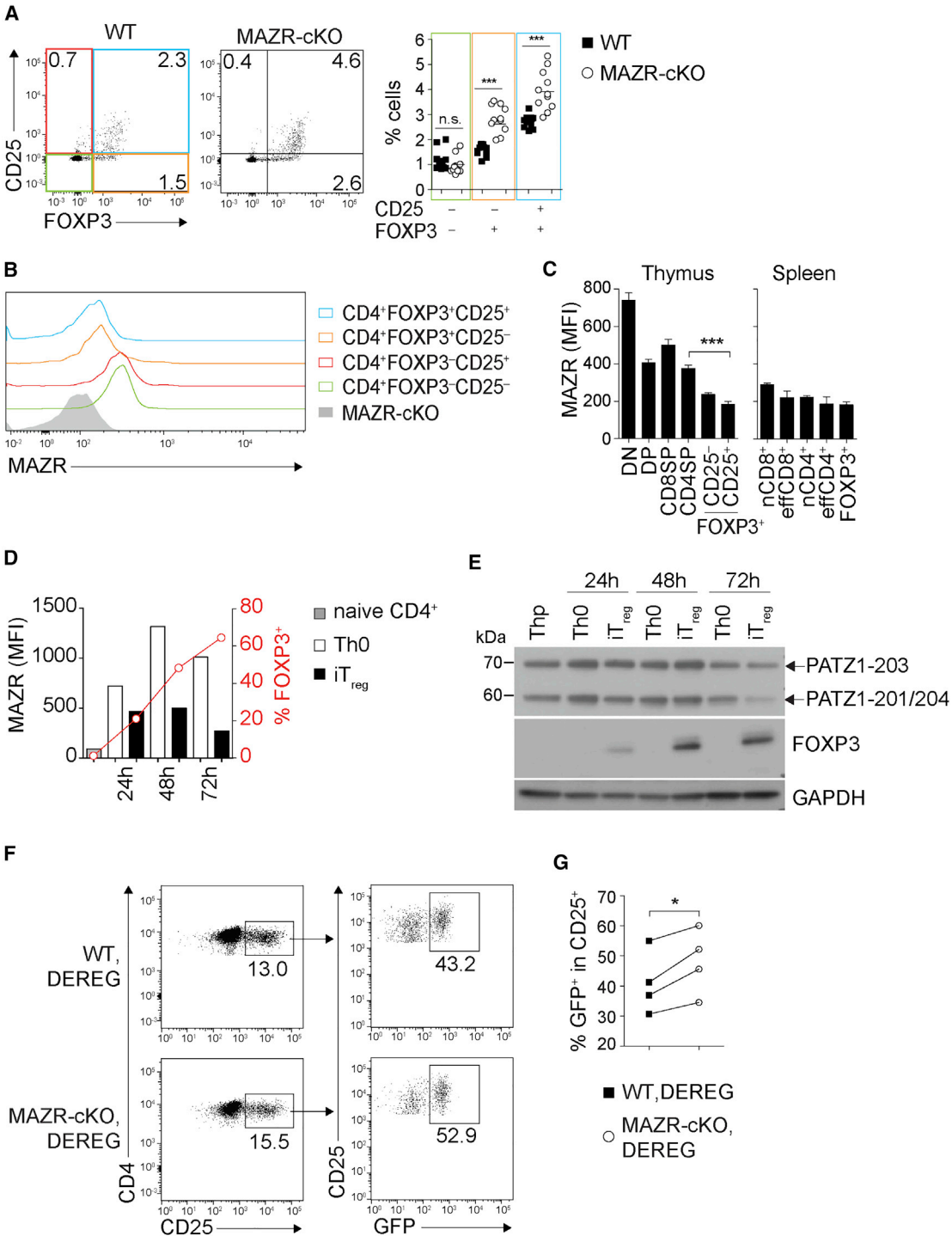

Figure 3. MAZR Affects Thymic T_{reg} Cell Development

(A) Dot plots depict CD25 and FOXP3 expression in WT and MAZR-cKO CD4SP thymocytes. Diagram (right) shows the percentages of $CD25^{-}FOXP3^{-}$, $CD25^{-}FOXP3^{+}$, and $CD25^{+}FOXP3^{+}$ cells, gated on CD4SP thymocytes, in WT and MAZR-cKO mice.

(B) Flow cytometry analysis shows MAZR expression in the indicated T cell subsets. The colored histograms show cells pre-gated on the four WT CD25 and FOXP3 quadrants from (A), depicting four different stages of tT_{reg} differentiation.

(C) Expression of MAZR was assessed by flow cytometry in DN, DP, CD8SP, CD4SP, $CD4^{+}CD25^{-}FOXP3^{+}$ (T_{reg} precursors), and $CD4^{+}CD25^{+}FOXP3^{+}$ (T_{reg}) subsets in the thymus as well as splenic $CD8^{+}CD44^{-}CD62L^{hi}$ (naive CD8), $CD8^{+}CD44^{+}CD62L^{-}$ (effector CD8), $CD4^{+}CD44^{-}CD62L^{hi}$ (naive CD4), $CD4^{+}CD44^{+}CD62L^{-}$ (effector CD4), and $CD4^{+}FOXP3^{+}$ (T_{reg}) subsets.

(legend continued on next page)

levels between FOXP3$^+$ and FOXP3$^-$ cells (Figure S2E), suggesting that MAZR expression levels alone are not decisive for the induction of FOXP3 in T cells cultured under iT$_{reg}$ cell-inducing conditions. A decrease in MAZR expression levels upon induction of FOXP3 expression was also observed in human T$_{reg}$ cell *in vitro* differentiation cultures (Figure 3E). Together, this indicates an inverse correlation of MAZR expression levels and FOXP3 induction in both murine and human T$_{reg}$ cells.

We next tested whether a loss of MAZR leads to an enhanced differentiation of FOXP3$^+$ T$_{reg}$ cells from CD4$^+$CD25$^+$FOXP3$^-$ progenitor cells in the thymus. Therefore, we sorted thymic TCRβ^{hi}CD4$^+$CD25$^+$EGFP$^-$ (i.e., FOXP3$^-$) populations from WT,DEREG and MAZR-cKO,DEREG mice, cultured the cells for 24 h with interleukin-2 (IL-2), and assessed the induction of FOXP3 expression using EGFP as a surrogate marker. In agreement with published studies (Kitagawa et al., 2017; Lio and Hsieh, 2008), a fraction of CD4$^+$CD25$^+$ WT cells remained CD25 positive and upregulated FOXP3 (i.e., EGFP). In the absence of MAZR, the percentage of CD4$^+$CD25$^+$ cells that induced FOXP3 (EGFP) expression was higher compared to WT cells (Figures 3F and 3G). This suggests that the increase in FOXP3$^+$ T$_{reg}$ cells by the loss of MAZR is, at least in part, due to their enhanced generation from thymic progenitors. CNS3 has been reported to function as a pioneer element in the initiation of *Foxp3* expression in T$_{reg}$ cells (Zheng et al., 2010). However, CNS3 does not, unlike CNS1 and CNS2, *trans*-activate reporter gene expression in primary CD4$^+$ T cells in transient luciferase assays (Schuster et al., 2012). In agreement with this study, we did not observe CNS3 activity in WT iT$_{reg}$ cells, and there was also no induction of CNS3 activity in MAZR-cKO iT$_{reg}$ cells (Figure S2F), indicating that MAZR is not responsible for restraining CNS3 transactivation activity under this experimental condition.

Enforced Expression of MAZR Leads to Impaired T$_{reg}$ Cell Differentiation

The observed downregulation of MAZR expression during tT$_{reg}$ cell differentiation suggests that low MAZR levels are essential for proper T$_{reg}$ cell development. To test this hypothesis, we overexpressed MAZR in developing thymocytes. Murine stem cell virus-based retroviral vectors containing *Mazr* (followed by an internal ribosomal entry site (IRES)-EGFP cassette to track transduced cells) (MAZR) or ''empty'' control (CTRL) vectors (Figure 4A) were used to infect hematopoietic stem cells, and, subsequently, transduced cells were transferred into recipient mice. After 6–8 weeks of reconstitution, the percentage of FOXP3$^+$ T cells within the transduced EGFP$^+$ thymocyte and splenocyte population was determined (Figure 4A). Within the EGFP$^+$ fraction of CD4SP thymocytes and CD4$^+$ splenocytes overexpressing MAZR, the percentage (Figures 4B and 4C) and numbers (Figure 4D) of FOXP3$^+$ CD4$^+$ T cells were reduced in comparison to the EGFP$^+$ fraction transduced with the control vector. Further, there was a tendency, although not statistically significant, of reduced FOXP3 expression levels (as revealed by MFI) in MAZR-transduced T$_{reg}$ cells in the thymus and spleen of BM chimeric mice (Figure 4E).

To test whether an enforced expression of MAZR also alters the generation of iT$_{reg}$ cells, we overexpressed MAZR during iT$_{reg}$ cell differentiation. For this, WT naive CD4$^+$ T cells were activated under iT$_{reg}$ cell-inducing conditions (in the presence of TGF-β) and transduced with MAZR and CTRL retroviral vectors (Figure 5A). Subsequently, the percentage of FOXP3$^+$ CD4$^+$ T cells within the EGFP$^+$ subsets (i.e., transduced cells) was determined. This revealed that the generation of iT$_{reg}$ cells was severely impaired upon overexpression of MAZR in a dose-dependent manner (Figures 5B and 5C). Of note, both the fraction of FOXP3$^+$ cells and the FOXP3 protein expression levels (MFI) in FOXP3$^+$ cells were significantly reduced (Figures 5C and 5D). This was due to transcriptional changes in *Foxp3* expression, since retroviral-mediated MAZR overexpression in WT,DEREG CD4$^+$ T cells (using a mCherry reporter cassette as readout for transduced cells) reduced the percentage of EGFP$^+$ (i.e., FOXP3$^+$) CD4$^+$ T cells (Figures S3A–S3C), as well as EGFP expression levels (based on the MFI of GFP$^+$ cells; Figure S3D). The reduction of FOXP3$^+$ iT$_{reg}$ cells was not due to an impaired proliferation of MAZR-overexpressing CD4$^+$ T cells, since MAZR- and CTRL-transduced CD4$^+$ T cells showed a similar rate of cell division (Figure 5E). Thus, enforced expression of MAZR impairs the development of tT$_{reg}$ cells as well as the differentiation of iT$_{reg}$ cells.

Minor Transcriptional Changes in MAZR-cKO T$_{reg}$ Cells

Our data demonstrate that MAZR regulates the differentiation of FOXP3$^+$ T$_{reg}$ cells. To investigate whether MAZR also controls the function of T$_{reg}$ cells, we first assessed the expression of several surface markers. The expression pattern of CD25, Nrp1, CD62L, CD44, CD69, CTLA-4, GITR, and KLRG1 on MAZR-cKO FOXP3$^+$ T$_{reg}$ cells was not different than that on WT FOXP3$^+$ T$_{reg}$ cells, indicating that there were no major alterations in the overall T$_{reg}$ cell subset distribution in the absence of MAZR under homeostatic conditions (Figure S4). To further characterize MAZR-deficient T$_{reg}$ cells on a genome-wide scale and to study potential transcriptional alterations in the absence of MAZR, we performed RNA-seq analysis of EGFP$^+$ T$_{reg}$ cells

(D) Naive CD4$^+$ T cells were activated under Th0 and iT$_{reg}$ cell-inducing conditions (using anti-CD3/anti-CD28 ± TGF-β). MAZR mean fluorescence intensity (MFI; left y axis, open and closed bars) and the percentage of FOXP3-expressing cells (%; right axis, red line) were assessed at day 0 (i.e., naive CD4$^+$), and after 24, 48, and 72 h.

(E) Immunoblot depicts MAZR (PATZ1) and FOXP3 expression in human CD4$^+$ T cells differentiated into Th0 and iT$_{reg}$ cells. GAPDH was used as a loading control.

(F) Sorted CD4$^+$CD25$^+$EGFP$^-$ thymocytes from WT,DEREG and MAZR-cKO,DEREG mice were cultured with IL-2 for 24 h and subjected to flow cytometric analysis to detect CD4, CD25 and EGFP expression.

(G) Diagram shows the percentages of EGFP$^+$ cells within WT,DEREG and MAZR-cKO,DEREG CD4$^+$CD25$^+$ T cells. Lines connect data points from the same experiments.

(A and F) Numbers indicate the percentage of cells in the respective quadrants or gates. Data are representative (A, B, and D–F) or show the summary (A, C, and G) of at least 25 (A), 4 (B and C), or 4 (E and F) mice, or of 2 experiments (D and E) that were analyzed in at least 15 (A), 2 (B–E), or 3 (F and G) independent experiments. *$p < 0.05$ and ***$p < 0.001$ (unpaired two-tailed Student's t test).

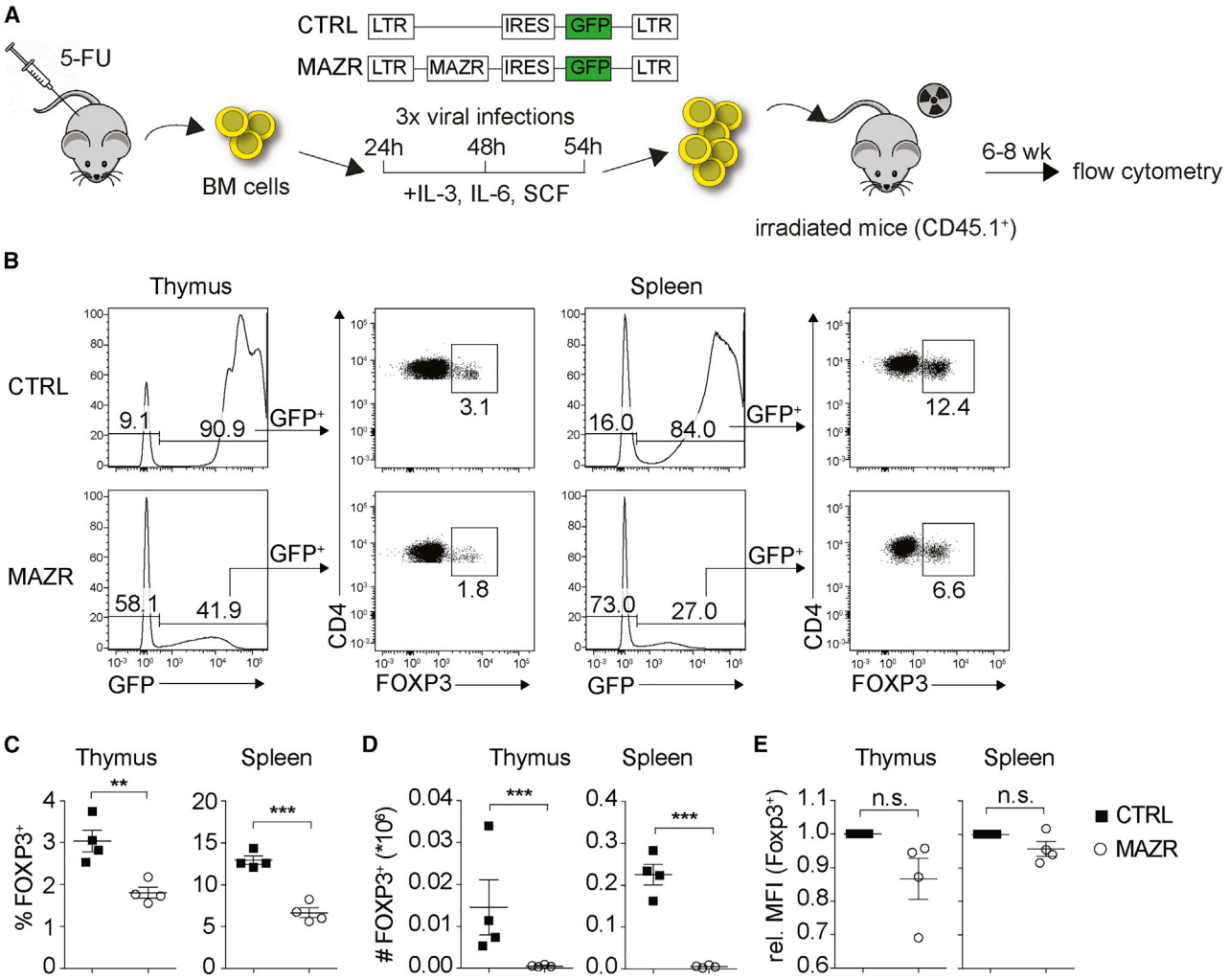

Figure 4. Enforced Expression of MAZR Impairs tT_{reg} Cell Generation *In Vivo*

(A) Experimental protocol: BM cells from 5-FU treated mice were isolated; cultured in the presence of IL-3, IL-6, and SCF; and infected with MAZR and "empty" control (CTRL) retrovirus. Transduced BM cells were injected into irradiated recipient mice, which were analyzed after 6–8 weeks via flow cytometry.

(B) Histograms to the left show the fraction of $EGFP^+$ thymocytes within MAZR and control vector transduced $CD45.2^+$ donor cells. Dot plots to the right depict CD4 and FOXP3 expression in $EGFP^+CD4SP$ thymocytes and $EGFP^+TCR\beta^+CD4^+$ splenocytes of mice reconstituted with BM transduced with MAZR and CTRL virus.

(C and D) Diagrams depict the percentages (C) and cell numbers (D) of $FOXP3^+$ cells from all experiments performed as in (B). The percentage of FOXP3-expressing transduced (i.e., $EGFP^+$) thymic CD4SP (left) and splenic $CD4^+$ T cells (right) is shown.

(E) Diagrams indicate the mean fluorescence intensity (MFI) of FOXP3 protein levels in $FOXP3^+$ CD4SP thymocytes (left) or splenic $FOXP3^+$ $CD4^+$ T cells (right) isolated from the transduced BM chimeric mice from all experiments performed as in (B). MFI levels in CTRL vector-transduced cells were set as 1, and relative MFI levels in MAZR-overexpressing cells are shown.

(B) Numbers indicate the percentage of cells in the respective gates. (C–E) Each symbol indicates one mouse. Horizontal bars indicate the mean. $^{**}p < 0.01$ and $^{***}p < 0.001$ (unpaired two-tailed Student's t test). Data are representative (B) or show the summary (C–E) of at least 4 mice (B–E) that were derived from 2 (B–E) independent BM transplantation experiments.

isolated from WT,DEREG and MAZR-cKO,DEREG mice. This revealed that 33 genes were upregulated, and 14 genes were downregulated in the absence of MAZR ($p \leq 0.05$; fold change [FC] ≥ 1.5) (Figures 6A and 6B). This low number of dysregulated genes suggests that MAZR only plays a minor role in establishing the transcriptional program of T_{reg} cells once the T_{reg} cell fate has been acquired.

Reduced Clinical Scores of DSS-Induced Colitis in MAZR-cKO Mice

The RNA-seq analysis indicated that a loss of MAZR only leads to minor changes in T_{reg} cell gene expression patterns. Nevertheless, to study whether a loss of MAZR has an impact on T_{reg} cell function, we applied both *in vitro* and *in vivo* methods to assess WT and MAZR-cKO T_{reg} cell suppressive activity under homeostatic

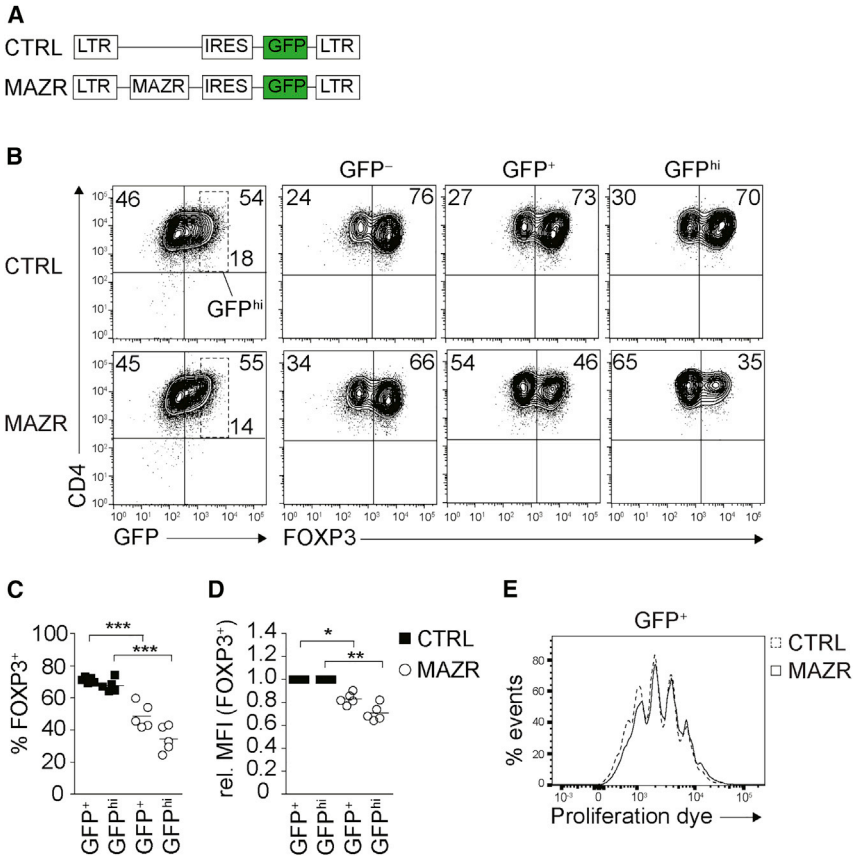

Figure 5. MAZR Overexpression Decreases iT$_{reg}$ Cell Differentiation

(A) Map of retroviral constructs used.

(B) Flow cytometry analysis shows CD4 and FOXP3 expression in CD4$^+$ T cells transduced with MAZR and CTRL retroviral vectors and polarized in the presence of TGF-β for 4 days. Plots are gated on viable and on EGFP$^-$, EGFP$^+$, and EGFP^{hi} populations, and the percentage of FOXP3$^+$ cells is shown.

(C and D) Diagrams show the percentages (C) and MFI (D) of FOXP3$^+$ cells within EGFP$^+$ and EGFP^{hi} cells of all experiments performed. MFI levels of CTRL-vector transduced iT$_{reg}$ cells were set as 1, and relative MFI levels in MAZR-overexpressing iT$_{reg}$ cells are shown.

(E) Flow cytometry analysis shows cell divisions of proliferation-dye-labeled EGFP$^+$ cells transduced as described in (B).

(B) Numbers indicate the percentage of cells in the respective quadrants or gates. (C and D) Each symbol indicates one independent experiment. Horizontal bars indicate the mean. *$p < 0.05$, **$p < 0.01$, and ***$p < 0.001$ (unpaired two-tailed Student's t test). Data are representative (B and E) or show the summary (C and D) of 5 (B–D) or 4 (E) independent experiments.

as well as diseased conditions. *In vitro* suppression assays indicated a slightly increased suppressive activity of splenic MAZR null FOXP3$^+$ T$_{reg}$ cells in comparison to splenic WT FOXP3$^+$ T$_{reg}$ cells (Figures 7A and 7B). However, we noted that the percentage of MAZR-cKO FOXP3$^+$ T cells at the end of in the suppression cultures was slightly higher compared to the WT cultures (Figures S5A and S5B). This might reflect an increased stability of FOXP3 expression in these cells, similar to reactivated MAZR-cKO iT$_{reg}$ cells (Figure 2F), and thus might contribute to the observed reduction in responder T cell proliferation.

To study whether the alteration in the T$_{reg}$ cell subset in MAZR-cKO mice has an impact on disease development *in vivo*, we applied an acute colitis model induced with DSS in WT and MAZR-cKO mice. This is a widespread model to analyze the function of innate as well as adaptive immunity in the setting of inflammatory bowel diseases (IBDs) (Wirtz et al., 2017), in which T$_{reg}$ cells have been shown to modulate disease severity (Boehm et al., 2012; Wang et al., 2015; Zhang et al., 2016). Upon administration of DSS, body weight was monitored and disease severity analyzed by colon histology (Figure 7C). MAZR-cKO mice displayed less weight loss as well as reduced histological scores in comparison to WT mice (Figures 7D–7F). This indicates that a T cell-specific loss of MAZR dampened DSS-induced disease severity *in vivo*.

To directly test MAZR-cKO T$_{reg}$ cell function *in vivo*, we also applied an adoptive T cell transfer model for colitis (Mottet et al., 2003) and transferred WT naive CD4$^+$ T cells together with either WT or MAZR-cKO T$_{reg}$ cells into RAG2-deficient hosts (Figure S6A). We did not observe any differences in disease severity with respect to body weight loss, colon length, and colon histology in recipient mice that received either WT or MAZR-cKO T$_{reg}$ cells (Figures S6B–S6D). This might suggest that the suppressive activity of T$_{reg}$ cells is not altered in the absence of MAZR in this preventive model of colitis. However, we noticed that the number of MAZR-cKO T$_{reg}$ cells in intestines of diseased mice was slightly reduced after transfer compared to WT T$_{reg}$ cell numbers (Figure S6E). This was clearly evident upon the transfer of only MAZR-cKO T$_{reg}$ cells into RAG2-deficient mice, since the percentage and number of MAZR-cKO T$_{reg}$ cells were significantly decreased 8 weeks after transfer compared to WT T$_{reg}$ cells in all lymphoid organs and cell subsets analyzed (spleen, mesenteric lymph nodes [mLNs], small intestinal intraepithelial lymphocytes (SI-IELs), small intestinal lamina propria lymphocytes (SI-LPLs) (Figures S6F and S6G). Moreover, we injected WT naive CD4$^+$ T cells (CD45.1$^+$) together with either WT or MAZR-cKO T$_{reg}$ cells into *Rag2*$^{-/-}$ hosts and assessed the expansion of conventional T cells and T$_{reg}$ cells in the spleens of recipient mice 7 days after transfer (Figure S7A), since T$_{reg}$ cells also control the homeostatic expansion of conventional T cells (Workman and Vignali, 2005). Again, the percentages of MAZR-cKO T$_{reg}$ cells were reduced compared to WT T$_{reg}$ cells, accompanied by a corresponding increase in conventional CD45.1$^+$CD4$^+$ T cells in the presence of MAZR-cKO T$_{reg}$ cells (Figures S7B and S7C). Together, these *in vivo* data suggest that MAZR-deficient T$_{reg}$ cells, upon transfer, display a different behavior compared to WT T$_{reg}$ cells.

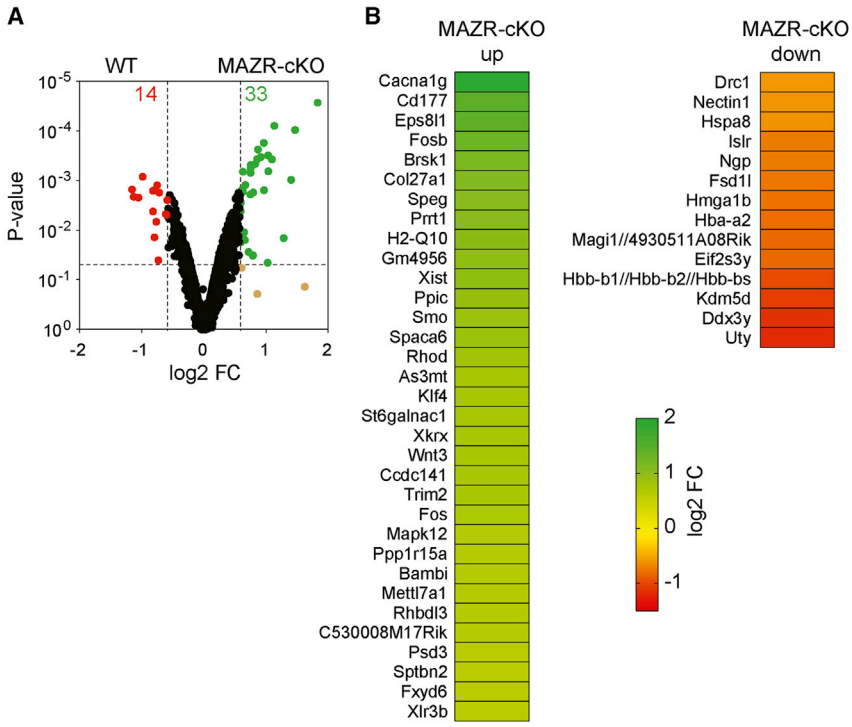

Figure 6. RNA Sequencing Reveals Minor Transcriptional Changes in the Absence of MAZR

(A) Volcano plot depicts gene expression in T_{reg} cells isolated from the spleens of WT,DEREG and MAZR-cKO,DEREG mice as revealed by RNA-seq. Cutoff lines of 1.5-fold change ($p \leq 0.05$) were applied to depict differentially expressed genes.

(B) Heatmap shows up- and downregulated genes in MAZR-cKO T_{reg} cells as defined in (A).

DISCUSSION

In this study, we demonstrate that the transcription factor MAZR/PATZ1 is a key modulator of FOXP3$^+$ T_{reg} cell development and differentiation. The observed increase in tT_{reg} cell development as well as the enhanced iT_{reg} cell differentiation from naive CD4$^+$ T cells in the absence of MAZR indicates a negative regulatory role for MAZR in the generation of the FOXP3$^+$ T_{reg} cell pool. Moreover, enforced expression of MAZR impairs T_{reg} cell differentiation in a dose-dependent manner, providing evidence that a tight control of MAZR expression levels is essential for proper T_{reg} cell differentiation. The finding that MAZR expression is downregulated during the development of FOXP3$^+$ T_{reg} cells supports these observations. The analysis of MAZR-deficient DEREG *Foxp3*-EGFP reporter mice also revealed an increase in the percentage of EGFP$^+$ cells, but not in EGFP protein expression levels, indicating that the increase in FOXP3$^+$ T_{reg} cells is due to an enhanced fraction of cells that expresses *Foxp3* mRNA and that the activation of the *Foxp3* gene locus is directly controlled by MAZR. We did not detect differences in the survival of WT and MAZR-cKO T_{reg} cells using AnnexinV and 7-AAD staining as a readout, suggesting that enhanced development rather than a preferential survival advantage leads to the elevated numbers of T_{reg} cells in the absence of MAZR. Indeed, we observed that MAZR deficiency promoted the induction of *Foxp3* expression in short-term cultured CD25$^+$FOXP3$^-$ CD4SP thymocytes, which are the progenitor cell population of FOXP3$^+$ T_{reg} cells (Burchill et al., 2008; Lio and Hsieh, 2008). *Foxp3* expression is, in addition to the promoter region, regulated by three major *cis*-regulatory elements designated as CNS1, CNS2, and CNS3 (Zheng et al., 2010). Among those, CNS2 is specifically demethylated in *ex vivo* isolated FOXP3$^+$ T_{reg} cells (TSDRs) (Floess et al., 2007). However, we observed no difference in the methylation status of CNS2 in the absence of MAZR; thus, it is rather unlikely that MAZR is part of the molecular machinery that controls the methylation status of the *Foxp3* gene in CD25$^+$FOXP3$^-$ CD4SP T_{reg} progenitor cells. CNS1, CNS2, and the *Foxp3* promoter (but not CNS3) display activity in activated CD4$^+$ T cells in transient luciferase transactivation assays (Polansky et al., 2010; Schuster et al., 2012). Since we did not detect differences between WT and MAZR-cKO iT_{reg} cells in the transactivation activity of CNS1, CNS2, or the *Foxp3* promoter, it is unlikely that MAZR directly controls the activity of these *cis*-elements. Unfortunately, currently available anti-MAZR/PATZ1 antibodies were not suitable for chromatin immunoprecipitation (ChIP)-PCR or ChIP sequencing (ChIP-seq) approaches in our hands; thus, it was not possible to study whether MAZR binds to other CNS regions within the *Foxp3* locus, such as CNS3, which functions as a pioneer element in regulating the induction of *Foxp3* expression (Zheng et al., 2010). We did not observe an induction of CNS3 activity in luciferase assays in the absence of MAZR; thus, MAZR is not responsible for restraining CNS3 activity. However, a loss of MAZR might facilitate an increased recruitment of factors such as c-Rel, which is required for tT_{reg} cell development (Isomura et al., 2009), to CNS3 and thereby promote enhanced T_{reg} cell development. Alternative approaches, such as the generation of ChIP-grade anti-MAZR antibodies or *in vivo* tagging of MAZR, would be required to determine whether MAZR is directly recruited to the *Foxp3* locus. These tools would also help to investigate a potential link between TGF-β signaling and MAZR in the generation of T_{reg} cells. TGF-β is crucial for the differentiation of tT_{reg} cells as well as iT_{reg} cells (Chen and Konkel, 2015), and both differentiation pathways are enhanced in the absence of MAZR. This raises the possibility that MAZR might be relevant in pathways downstream of TGFβ signaling, leading to the induction of *Foxp3* expression. Interestingly, although MAZR was expressed at lower levels in T_{reg} cells activated in the presence of TGF-β, compared to solely anti-CD3/anti-CD28 cultured CD4$^+$ T cells, we did not observe differences in MAZR protein levels between FOXP3$^+$ and FOXP3$^-$ cells in iT_{reg} cultures. This suggests that the expression level of MAZR alone

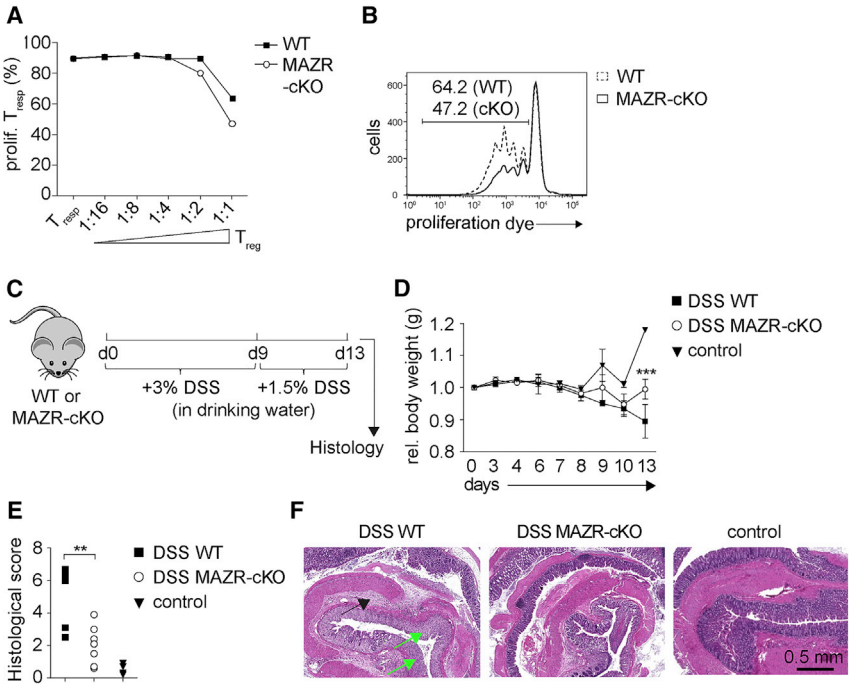

Figure 7. MAZR-cKO Mice Exhibit Reduced Disease Scores in DSS-Induced Colitis

(A) Diagram shows the percentage of proliferated CD45.1$^+$ CD4$^+$ responder T cells (T_{resp} cells) that were cultured in the presence of antigen-presenting cells, anti-CD3, and TGF-β for 3 days at different ratios with FACS-purified CD45.2$^+$ EGFP$^+$ WT,DEREG or MAZR-cKO,DEREG T_{reg} cells.

(B) Histogram depicts cell proliferation at a 1:1 T_{reg} to T_{resp} cell ratio.

(C) Experimental scheme of the DSS-induced colitis disease model.

(D) Diagram depicts the mean of the relative body weight loss upon colitis induction.

(E) Diagram depicts the histological disease severity score according to crypt damage, inflammatory cell infiltration, epithelial erosion, and goblet cell depletion of all mice analyzed.

(F) H&E staining of representative swiss roll slides of the distal colon from WT,DEREG or MAZR-cKO,-DEREG mice treated with DSS (or untreated controls) as described. Arrows point to highly inflamed areas with damaged crypts (green arrows) and epithelial erosion (black arrow).

Data are representative (A, B, and F) of 3 (A and B) or 2 (F) independent experiments or show the summary (D and E) of at least 7 mice that were analyzed in at least 2 independent experiments. In (E), each symbol indicates one mouse. $^{**}p < 0.01$ and $^{***}p < 0.001$ (unpaired two-tailed Student's t test). H_2O control: WT mice that received normal drinking water. The bar indicates 0.5 mm.

is not decisive for the induction of FOXP3 expression in iT$_{reg}$ cells. This might indicate that MAZR restricts iT$_{reg}$ cell differentiation together with a network of other factors that might be differentially expressed in FOXP3$^+$ and FOXP3$^-$ cells. Alternatively, it is also conceivable that MAZR regulates FOXP3 via chromatin-mediated effects and that a loss of MAZR increases the probability that *Foxp3* expression is induced. We observed similar effects at the *Cd8ab* gene locus, since the loss of MAZR partially reverted a CD8 expression variegation phenotype upon the combined deletion of *Cd8* enhancers E8-I and E8-II (Sakaguchi et al., 2010), or on the *Zbtb7b* locus (encoding for ThPOK), since a fraction of MAZR-deficient CD8$^+$ T cells derepressed ThPOK (Sakaguchi et al., 2010, 2015). Of note, the transcription factor ThPOK has been shown to promote T$_{reg}$ cell development (Carpenter et al., 2017; Twu and Teh, 2014). Moreover, MAZR represses the *Zbtb7b* locus in MHC class-I-signaled DP thymocytes (Sakaguchi et al., 2010). However, by analyzing WT and MAZR-cKO mice that were crossed to ThPOK-GFP reporter mice (Setoguchi et al., 2008), we did not observe an alteration in *Zbtb7b* expression CD4$^+$ T cells or in T$_{reg}$ cells (data not shown), indicating that MAZR does not modulate iT$_{reg}$ cell development by restricting ThPOK expression.

Our data demonstrate that MAZR regulates T$_{reg}$ cell development and differentiation. However, the deletion of MAZR led to a rather low number of transcriptional changes in *ex vivo* analyzed FOXP3$^+$ T$_{reg}$ cells, indicating a minor role for MAZR in maintaining the transcriptional program in T$_{reg}$ cells once the T$_{reg}$ cell fate has been acquired. Alternatively, other factors might compensate for a loss of MAZR in T$_{reg}$ cells, similar to the observation in DP thymocytes, where the combined deletion of MAZR and Runx1 resulted in the derepression of ThPOK, which was not seen upon individual deletion (Sakaguchi et al., 2015). Further, the observation that FOXP3$^+$ T$_{reg}$ cells display only a mildly enhanced *in vitro* suppressive function suggests a minor role for MAZR in controlling T$_{reg}$ cell activity. Nevertheless, evidence for a functional role of MAZR is obtained from an acute DSS-induced colitis model, in which T$_{reg}$ cells have previously been described to reduce disease severity (Boehm et al., 2012; Wang et al., 2015; Zhang et al., 2016). We observed an amelioration of DSS-induced disease severity in MAZR-cKO mice, which might be due to elevated numbers of T$_{reg}$ cells under homeostatic conditions or, in line with the enhanced *in vitro* suppressive activity of MAZR-cKO T$_{reg}$ cells, to an altered function of MAZR-cKO T$_{reg}$ cells. Although there was no difference in IFNγ or IL-17A production between *in vitro* differentiated WT and MAZR-cKO Th1 or Th17 cells, respectively (data not shown), we cannot formally exclude that the reduced disease severity was due to a weakened *in vivo* effector function of Th subsets in MAZR-cKO mice. Thus, further studies applying T$_{reg}$ cell-specific deletion of MAZR are required to determine whether MAZR alters T$_{reg}$ function in DSS-induced colitis.

Nevertheless, we would argue that MAZR controls T$_{reg}$ cell biology *in vivo*. We observed a reduction of MAZR-cKO T$_{reg}$ cells after a transfer into RAG2-deficient mice in comparison to transferred WT T$_{reg}$ cells. Several possibilities can be envisaged why the loss of MAZR changes T$_{reg}$ cells *in vivo*: alterations in their

ability to properly expand, a reduced survival upon expansion, or an impaired migration to target tissues in the setting of disease. Thus, a potentially increased suppressive activity of MAZR-cKO T_{reg} cells that would reduce disease severity in the adoptive T cell transfer colitis model might be masked by the reduced numbers of T_{reg} cells upon transfer. Further studies that include monitoring the fate of MAZR-deficient T_{reg} cells upon transfer are required to address these issues. One additional possibility of how a loss of MAZR affects T_{reg} cells *in vivo* might be provided by the observation that MAZR is part of the FOXP3 interactome (Rudra et al., 2012). FOXP3 regulates target genes and transcriptional programs in T_{reg} cells through several independent mechanisms (Marson et al., 2007; Zheng et al., 2007), in many cases by interactions with other transcription factors (Xie et al., 2015). Thus, MAZR might co-regulate the expression of some FOXP3 target genes, which are potentially altered upon the activation/expansion of T_{reg} cells *in vivo* in the absence of MAZR. Further studies that include RNA-seq analysis of *in vivo* activated WT and MAZR-cKO T_{reg} cells are required to address transcriptional changes *in vivo* as well as a potential co-regulation of FOXP3 target genes by MAZR.

Taken together, our data indicate that MAZR is part of the transcriptional network modulating T_{reg} cell development and that MAZR controls the generation of the T_{reg} cell pool under homeostatic conditions. Therefore, targeting MAZR expression levels might be a strategy for fine-tuning T_{reg} cell numbers under certain disease conditions.

STAR★METHODS

Detailed methods are provided in the online version of this paper and include the following:

- KEY RESOURCES TABLE
- LEAD CONTACT AND MATERIALS AVAILABILITY
- EXPERIMENTAL MODEL AND SUBJECT DETAILS
  - Human samples
  - Mice
- METHOD DETAILS
  - Genotyping of mice
  - T cell isolation, T cell stimulation, iT_{reg} cultures and intracellular staining
  - Flow cytometry and antibodies
  - Retroviral infection of $CD4^+$ T_{reg} cells
  - Generation of bone marrow (BM) reconstituted mice
  - tT_{reg} differentiation cultures
  - Suppression assays
  - Bisulphite sequencing
  - Immunoblot analysis
  - Synthesis of cDNA and qRTPCR
  - *In vitro* luciferase reporter assays
  - DSS-induced colitis and T cell isolation from small intestine
  - Adoptive T cell transfer colitis
  - Homeostatic T cell expansion upon adoptive transfer
  - RNA-Sequencing and sample preparation
  - Human $CD4^+$ T cell isolation and differentiation into iT_{reg} cells
- QUANTIFICATION AND STATISTICAL ANALYSIS
  - Bioinformatic analysis of RNA-sequencing data
  - Statistical analysis
- DATA AND CODE AVAILABILITY

SUPPLEMENTAL INFORMATION

Supplemental Information can be found online at https://doi.org/10.1016/j.celrep.2019.11.089.

ACKNOWLEDGMENTS

We thank the Biomedical Sequencing Facility at CeMM for assistance with next-generation sequencing. We thank Dr. Ubaid Ullah for insightful discussions and Marjo Hakkarainen and Sarita Heinonen, Turku Centre for Biotechnology, for excellent technical assistance. We are grateful for the support from Biocenter Finland and ELIXIR Finland node hosted at CSC - IT Center for Science for ICT resources. W.E. was supported by the Austrian Science Fund (FWF) projects P23641, P26193, P29790, and I00698; the FWF special research program SFB F70; and by the FWF and Medical University of Vienna doctoral programs (DK W1212) "Inflammation and Immunity" and (DOC 32 doc.fund) "TissueHome". S.S. was supported by FWF project P27747. J.H. was supported by the German Research Foundation (SFB738). L.L.E. was supported by the European Research Council ERC (677943); the Academy of Finland (296801, 304995, 310561 and 313343); the Juvenile Diabetes Research Foundation JDRF (2-2013-32); the Sigrid Juselius Foundation; the University of Turku, Åbo Akademi University; the Turku Graduate School (UTUGS); the Biocenter Finland; and by ELIXIR Finland. R.L. was supported by the Academy of Finland (AoF) Centre of Excellence in Molecular Systems Immunology and Physiology Research (2012–2017) grant 250114; the AoF grants 292335, 294337, 292482, 319280 and 31444; the Sigrid Jusélius Foundation; and by the Finnish Cancer Foundation. W.E., J.H., and L.L.E. were supported by the European Union's Horizon 2020 Research and Innovation Program (ENLIGHT-TEN Innovative Training Network under the Marie Skłodowska-Curie grant agreement 675395).

AUTHOR CONTRIBUTIONS

L.A., A.F.G., M.A., T.P., M.J.O., N.D., V.S., A.S., A.H., S.F., and S.B.A.A. performed experiments and analyzed the data. S.S. generated floxed MAZR mice. P.H., S.S., S.K., S.F., J.H., O.R., and R.L. analyzed data. T.K., C.B., T.F., L.L.E., and A.L. performed the bioinformatics analysis. T.S. provided mice. L.A. and W.E. designed the research, analyzed data, and wrote the manuscript.

DECLARATION OF INTERESTS

The authors declare no competing interests.

Received: November 30, 2018
Revised: October 24, 2019
Accepted: November 21, 2019
Published: December 24, 2019

REFERENCES

Abramova, A., Sakaguchi, S., Schebesta, A., Hassan, H., Boucheron, N., Valent, P., Roers, A., and Ellmeier, W. (2013). The transcription factor MAZR preferentially acts as a transcriptional repressor in mast cells and plays a minor role in the regulation of effector functions in response to FcεRI stimulation. PLoS ONE *8*, e77677.

Andrews, S. (2010). FastQC: a quality control tool for high throughput sequence data, Available online at. http://www.bioinformatics.babraham.ac.uk/projects/fastqc.

Bilic, I., Koesters, C., Unger, B., Sekimata, M., Hertweck, A., Maschek, R., Wilson, C.B., and Ellmeier, W. (2006). Negative regulation of CD8 expression via

Cd8 enhancer-mediated recruitment of the zinc finger protein MAZR. Nat. Immunol. *7*, 392–400.

Boehm, F., Martin, M., Kesselring, R., Schiechl, G., Geissler, E.K., Schlitt, H.J., and Fichtner-Feigl, S. (2012). Deletion of Foxp3+ regulatory T cells in genetically targeted mice supports development of intestinal inflammation. BMC Gastroenterol. *12*, 97.

Boucheron, N., Tschismarov, R., Goeschl, L., Moser, M.A., Lagger, S., Sakaguchi, S., Winter, M., Lenz, F., Vitko, D., Breitwieser, F.P., et al. (2014). CD4(+) T cell lineage integrity is controlled by the histone deacetylases HDAC1 and HDAC2. Nat. Immunol. *15*, 439–448.

Burchill, M.A., Yang, J., Vang, K.B., Moon, J.J., Chu, H.H., Lio, C.W., Vegoe, A.L., Hsieh, C.S., Jenkins, M.K., and Farrar, M.A. (2008). Linked T cell receptor and cytokine signaling govern the development of the regulatory T cell repertoire. Immunity *28*, 112–121.

Carpenter, A.C., Wohlfert, E., Chopp, L.B., Vacchio, M.S., Nie, J., Zhao, Y., Shetty, J., Xiao, Q., Deng, C., Tran, B., et al. (2017). Control of Regulatory T Cell Differentiation by the Transcription Factors Thpok and LRF. J. Immunol. *199*, 1716–1728.

Chen, W., and Konkel, J.E. (2015). Development of thymic Foxp3(+) regulatory T cells: TGF-β matters. Eur. J. Immunol. *45*, 958–965.

Curotto de Lafaille, M.A., and Lafaille, J.J. (2009). Natural and adaptive foxp3+ regulatory T cells: more of the same or a division of labor? Immunity *30*, 626–635.

Dobin, A., Davis, C.A., Schlesinger, F., Drenkow, J., Zaleski, C., Jha, S., Batut, P., Chaisson, M., and Gingeras, T.R. (2013). STAR: ultrafast universal RNA-seq aligner. Bioinformatics *29*, 15–21.

Floess, S., Freyer, J., Siewert, C., Baron, U., Olek, S., Polansky, J., Schlawe, K., Chang, H.D., Bopp, T., Schmitt, E., et al. (2007). Epigenetic control of the foxp3 locus in regulatory T cells. PLoS Biol. *5*, e38.

Fontenot, J.D., Gavin, M.A., and Rudensky, A.Y. (2003). Foxp3 programs the development and function of CD4+CD25+ regulatory T cells. Nat. Immunol. *4*, 330–336.

Gentleman, R.C., Carey, V.J., Bates, D.M., Bolstad, B., Dettling, M., Dudoit, S., Ellis, B., Gautier, L., Ge, Y., Gentry, J., et al. (2004). Bioconductor: open software development for computational biology and bioinformatics. Genome Biol. *5*, R80.

Hawkins, R.D., Larjo, A., Tripathi, S.K., Wagner, U., Luu, Y., Lönnberg, T., Raghav, S.K., Lee, L.K., Lund, R., Ren, B., et al. (2013). Global chromatin state analysis reveals lineage-specific enhancers during the initiation of human T helper 1 and T helper 2 cell polarization. Immunity *38*, 1271–1284.

Hori, S., Nomura, T., and Sakaguchi, S. (2003). Control of regulatory T cell development by the transcription factor Foxp3. Science *299*, 1057–1061.

Huehn, J., and Beyer, M. (2015). Epigenetic and transcriptional control of Foxp3+ regulatory T cells. Semin. Immunol. *27*, 10–18.

Isomura, I., Palmer, S., Grumont, R.J., Bunting, K., Hoyne, G., Wilkinson, N., Banerjee, A., Proietto, A., Gugasyan, R., Wu, L., et al. (2009). c-Rel is required for the development of thymic Foxp3+ CD4 regulatory T cells. J. Exp. Med. *206*, 3001–3014.

Josefowicz, S.Z., Lu, L.F., and Rudensky, A.Y. (2012). Regulatory T cells: mechanisms of differentiation and function. Annu. Rev. Immunol. *30*, 531–564.

Khattri, R., Cox, T., Yasayko, S.A., and Ramsdell, F. (2003). An essential role for Scurfin in CD4+CD25+ T regulatory cells. Nat. Immunol. *4*, 337–342.

Kitagawa, Y., and Sakaguchi, S. (2017). Molecular control of regulatory T cell development and function. Curr. Opin. Immunol. *49*, 64–70.

Kitagawa, Y., Ohkura, N., Kidani, Y., Vandenbon, A., Hirota, K., Kawakami, R., Yasuda, K., Motooka, D., Nakamura, S., Kondo, M., et al. (2017). Guidance of regulatory T cell development by Satb1-dependent super-enhancer establishment. Nat. Immunol. *18*, 173–183.

Lahl, K., Loddenkemper, C., Drouin, C., Freyer, J., Arnason, J., Eberl, G., Hamann, A., Wagner, H., Huehn, J., and Sparwasser, T. (2007). Selective depletion of Foxp3+ regulatory T cells induces a scurfy-like disease. J. Exp. Med. *204*, 57–63.

Lee, P.P., Fitzpatrick, D.R., Beard, C., Jessup, H.K., Lehar, S., Makar, K.W., Pérez-Melgosa, M., Sweetser, M.T., Schlissel, M.S., Nguyen, S., et al. (2001). A critical role for Dnmt1 and DNA methylation in T cell development, function, and survival. Immunity *15*, 763–774.

Li, X., and Zheng, Y. (2015). Regulatory T cell identity: formation and maintenance. Trends Immunol. *36*, 344–353.

Liao, Y., Smyth, G.K., and Shi, W. (2014). featureCounts: an efficient general purpose program for assigning sequence reads to genomic features. Bioinformatics *30*, 923–930.

Lio, C.W., and Hsieh, C.S. (2008). A two-step process for thymic regulatory T cell development. Immunity *28*, 100–111.

Marson, A., Kretschmer, K., Frampton, G.M., Jacobsen, E.S., Polansky, J.K., MacIsaac, K.D., Levine, S.S., Fraenkel, E., von Boehmer, H., and Young, R.A. (2007). Foxp3 occupancy and regulation of key target genes during T-cell stimulation. Nature *445*, 931–935.

Moolenbeek, C., and Ruitenberg, E.J. (1981). The "Swiss roll": a simple technique for histological studies of the rodent intestine. Lab. Anim. *15*, 57–59.

Mottet, C., Uhlig, H.H., and Powrie, F. (2003). Cutting edge: cure of colitis by CD4+CD25+ regulatory T cells. J. Immunol. *170*, 3939–3943.

Polansky, J.K., Schreiber, L., Thelemann, C., Ludwig, L., Krüger, M., Baumgrass, R., Cording, S., Floess, S., Hamann, A., and Huehn, J. (2010). Methylation matters: binding of Ets-1 to the demethylated Foxp3 gene contributes to the stabilization of Foxp3 expression in regulatory T cells. J. Mol. Med. (Berl.) *88*, 1029–1040.

Robinson, M.D., McCarthy, D.J., and Smyth, G.K. (2010). edgeR: a Bioconductor package for differential expression analysis of digital gene expression data. Bioinformatics *26*, 139–140.

R Team. (2015). R: A Language and Environment for Statistical Computing. R Foundation for Statistical Computing, *1*, p. 409.

Rudra, D., deRoos, P., Chaudhry, A., Niec, R.E., Arvey, A., Samstein, R.M., Leslie, C., Shaffer, S.A., Goodlett, D.R., and Rudensky, A.Y. (2012). Transcription factor Foxp3 and its protein partners form a complex regulatory network. Nat. Immunol. *13*, 1010–1019.

Sakaguchi, S., Hombauer, M., Bilic, I., Naoe, Y., Schebesta, A., Taniuchi, I., and Ellmeier, W. (2010). The zinc-finger protein MAZR is part of the transcription factor network that controls the CD4 versus CD8 lineage fate of double-positive thymocytes. Nat. Immunol. *11*, 442–448.

Sakaguchi, S., Hainberger, D., Tizian, C., Tanaka, H., Okuda, T., Taniuchi, I., and Ellmeier, W. (2015). MAZR and Runx Factors Synergistically Repress ThPOK during CD8+ T Cell Lineage Development. J. Immunol. *195*, 2879–2887.

Schlenner, S.M., Weigmann, B., Ruan, Q., Chen, Y., and von Boehmer, H. (2012). Smad3 binding to the foxp3 enhancer is dispensable for the development of regulatory T cells with the exception of the gut. J. Exp. Med. *209*, 1529–1535.

Schuster, M., Glauben, R., Plaza-Sirvent, C., Schreiber, L., Annemann, M., Floess, S., Kühl, A.A., Clayton, L.K., Sparwasser, T., Schulze-Osthoff, K., et al. (2012). IκB(NS) protein mediates regulatory T cell development via induction of the Foxp3 transcription factor. Immunity *37*, 998–1008.

Setoguchi, R., Tachibana, M., Naoe, Y., Muroi, S., Akiyama, K., Tezuka, C., Okuda, T., and Taniuchi, I. (2008). Repression of the transcription factor Th-POK by Runx complexes in cytotoxic T cell development. Science *319*, 822–825.

Suomi, T., Seyednasrollah, F., Jaakkola, M.K., Faux, T., and Elo, L.L. (2017). ROTS: An R package for reproducibility-optimized statistical testing. PLoS Comput. Biol. *13*, e1005562.

Tai, X., Erman, B., Alag, A., Mu, J., Kimura, M., Katz, G., Guinter, T., McCaughtry, T., Etzensperger, R., Feigenbaum, L., et al. (2013). Foxp3 transcription factor is proapoptotic and lethal to developing regulatory T cells unless counterbalanced by cytokine survival signals. Immunity *38*, 1116–1128.

Toker, A., Engelbert, D., Garg, G., Polansky, J.K., Floess, S., Miyao, T., Baron, U., Düber, S., Geffers, R., Giehr, P., et al. (2013). Active demethylation of the Foxp3 locus leads to the generation of stable regulatory T cells within the thymus. J. Immunol. *190*, 3180–3188.

Tone, Y., Furuuchi, K., Kojima, Y., Tykocinski, M.L., Greene, M.I., and Tone, M. (2008). Smad3 and NFAT cooperate to induce Foxp3 expression through its enhancer. Nat. Immunol. *9*, 194–202.

Twu, Y.C., and Teh, H.S. (2014). The ThPOK transcription factor differentially affects the development and function of self-specific CD8(+) T cells and regulatory CD4(+) T cells. Immunology *141*, 431–445.

Ullah, U., Andrabi, S.B.A., Tripathi, S.K., Dirasantha, O., Kanduri, K., Rautio, S., Gross, C.C., Lehtimäki, S., Bala, K., Tuomisto, J., et al. (2018). Transcriptional Repressor HIC1 Contributes to Suppressive Function of Human Induced Regulatory T Cells. Cell Rep. *22*, 2094–2106.

van der Veeken, J., Arvey, A., and Rudensky, A. (2013). Transcriptional control of regulatory T-cell differentiation. Cold Spring Harb. Symp. Quant. Biol. *78*, 215–222.

Wang, L., Ray, A., Jiang, X., Wang, J.Y., Basu, S., Liu, X., Qian, T., He, R., Dittel, B.N., and Chu, Y. (2015). T regulatory cells and B cells cooperate to form a regulatory loop that maintains gut homeostasis and suppresses dextran sulfate sodium-induced colitis. Mucosal Immunol. *8*, 1297–1312.

Williams, L.M., and Rudensky, A.Y. (2007). Maintenance of the Foxp3-dependent developmental program in mature regulatory T cells requires continued expression of Foxp3. Nat. Immunol. *8*, 277–284.

Wirtz, S., Popp, V., Kindermann, M., Gerlach, K., Weigmann, B., Fichtner-Feigl, S., and Neurath, M.F. (2017). Chemically induced mouse models of acute and chronic intestinal inflammation. Nat. Protoc. *12*, 1295–1309.

Workman, C.J., and Vignali, D.A. (2005). Negative regulation of T cell homeostasis by lymphocyte activation gene-3 (CD223). J. Immunol. *174*, 688–695.

Xie, X., Stubbington, M.J., Nissen, J.K., Andersen, K.G., Hebenstreit, D., Teichmann, S.A., and Betz, A.G. (2015). The Regulatory T Cell Lineage Factor Foxp3 Regulates Gene Expression through Several Distinct Mechanisms Mostly Independent of Direct DNA Binding. PLoS Genet. *11*, e1005251.

Zhang, H.L., Zheng, Y.J., Pan, Y.D., Xie, C., Sun, H., Zhang, Y.H., Yuan, M.Y., Song, B.L., and Chen, J.F. (2016). Regulatory T-cell depletion in the gut caused by integrin β7 deficiency exacerbates DSS colitis by evoking aberrant innate immunity. Mucosal Immunol. *9*, 391–400.

Zheng, Y., Josefowicz, S.Z., Kas, A., Chu, T.T., Gavin, M.A., and Rudensky, A.Y. (2007). Genome-wide analysis of Foxp3 target genes in developing and mature regulatory T cells. Nature *445*, 936–940.

Zheng, Y., Josefowicz, S., Chaudhry, A., Peng, X.P., Forbush, K., and Rudensky, A.Y. (2010). Role of conserved non-coding DNA elements in the Foxp3 gene in regulatory T-cell fate. Nature *463*, 808–812.

STAR★METHODS

KEY RESOURCES TABLE

REAGENT or RESOURCE	SOURCE	IDENTIFIER
Antibodies		
CD3 purified NA/LE(145-2C11)	BD Biosciences	Cat# 553057; RRID: AB_394590
CD4-PE-Cy7 (RM4-5)	eBioscience	Cat#25-0042-82; RRID: AB_469578
CD8a-PerCP-Cy5.5 (53-6.7)	BD Biosciences	Cat#551162; RRID: AB_394081
CD19-FITC (1D3)	BD Biosciences	Cat# 557398; RRID: AB_396681
CD24-PE (M1/69)	BioLegend	Cat# 101807; RRID: AB_312840
CD25-PE (PC61 5.3 7)	BD Biosciences	Cat#553866; RRID: AB_395101
CD28 purified NA/LE (37.51)	BD Biosciences	Cat# 553294; RRID: AB_394763
CD44-BV421 (IM7)	BioLegend	Cat# 103040; RRID: AB_2616903
CD45.1-PE/Dazzle594 (A20)	BioLegend	Cat#110748; RRID: AB_2564295
CD45.2-PerCP-Cy5.5 (104)	eBioscience	Cat#45-0454-82; RRID: AB_953590
CD45R-BV605 (RA3-6B2)	BioLegend	Cat# 103243; RRID: AB_11203907
CD69-V450 (H1.2F3)	BD Biosciences	Cat# 560690; RRID: AB_1727511
FoxP3-APC (FJK-16 s)	eBioscience	Cat# 17-5773-82; RRID: AB_469457
FoxP3-PE (FJK-16 s)	eBioscience	Cat# 12-5773-82; RRID: AB_465936
TCRb-APC-eFluor 780 (H57-597)	eBioscience	Cat# 47-5961-82; RRID: AB_1272173
CD11b-biotin (M1/70)	Biolegend	Cat# 101204; RRID: AB_312787
CD11c-biotin (HL3)	Biolegend	Cat# 117304; RRID: AB_313773
CD62L-BV605 (MEL-14)	Biolegend	Cat# 104438; RRID: AB_2563058
CD103-BV421 (2E7)	Biolegend	Cat# 121521; RRID: AB_10900074
CD134/Ox40-PE (OX-86)	Biolegend	Cat# 119409; RRID: AB_2272150
CD152/CTLA4-PE (UC10-4B9)	Biolegend	Cat# 106305; RRID: AB_313254
CD154/CD40L-APC (MR1)	eBioscience	Cat# 17-1541-82; RRID: AB_795823
Gr-1-biotin (RB6-8C5)	Biolegend	Cat# 108404; RRID: AB_313369
Nur77-PE (12.14)	eBioscience	Cat# 12-5965-80; RRID: AB_1257209
NK1.1-biotin (PK136)	Biolegend	Cat# 108704; RRID: AB_313391
Ter119-biotin (TER-119)	Biolegend	Cat# 116204; RRID: AB_313705
IL-10-PE (JESS-16E3)	Biolegend	Cat# 505007; RRID: AB_315361
Helios-FITC (22F6)	Biolegend	Cat# 137204; RRID: AB_10549181
Patz1 (Clone 31)	abcam	Cat# ab191448
Patz1 (D-5)	Santa Cruz	Cat# sc-390577
IgG1-AF647 (RMG1-1)	Biolegend	Cat# 406618; RRID: AB_2563477
anti-human FOXP3 (PCH101)	eBioscience	Cat# 14-4776-82; RRID: AB_467554
GAPDH (6C5)	HyTest	Cat# 5G4; RRID: AB_1616722
TrueBlot ULTRA: Anti-Mouse Ig HRP (eB144)	Rockland Immunochemicals	Cat# 18-8817-33; RRID: AB_2610851
CD8a-APC (53-6.7)	eBioscience	Cat# 17-0081-83; RRID: AB_469335
CD90.2-BV605 (53-2.1)	BioLegend	Cat# 140318; RRID: AB_2650924
CD8b-PE (H35-17.2)	BD Biosciences	Cat# 550798; RRID: AB_393887
GITR-PE-Cy7 (YGITR 765)	BioLegend	Cat# 120222; RRID: AB_528907
Qa2-AF647 (695H1-9-9)	BioLegend	Cat# 121708; RRID: AB_571989
CD8a-biotin (53-6.7)	BioLegend	Cat# 100704; RRID: AB_312743
CD44-AF700 (IM7)	BioLegend	Cat# 103026; RRID: AB_493713

(*Continued on next page*)

Continued

REAGENT or RESOURCE	SOURCE	IDENTIFIER
Bacterial and Virus Strains		
DH5a competent cells	N/A	N/A
Chemicals, Peptides, and Recombinant Proteins		
RPMI1640	Sigma Aldrich	R8758
FCS	Sigma Aldrich	F7524-500ML
b-mercaptoethanol	Sigma Aldrich	M3148-25ML
TGF-b	R&D Systems	240-B-002
PMA (phorbol 12-myristate 13-acetate)	Sigma Aldrich	P8139
Ionomycin calcium salt	Sigma Aldrich	I3909
Polybrene (Hexadimethrine bromide)	Sigma Aldrich	H9268
GlutaMAX	Life Technologies	35050038
DNaseI	Life Technologies	EN0521
SuperScriptIII reverse transcriptase	Invitrogen	10368252
iTag Universal SYBR Green	BioRad	Cat# 172-5121
DSS (Dextrane Sulfate Sodium)	Sigma Aldrich	42867
PFA (Para-formaldehyde)	Sigma Aldrich	158127-500G
EDTA	Roth	X986.2
Collagenase Type II	GIBCO	17101015
Percoll	Sigma Aldrich	17-0891-02
Critical Commercial Assays		
BD Cytofix/Cytoperm	BD Biosciences	Cat# 554722
FOXP3/Transcription Factor Staining Buffer Set	eBioscience	Cat# 00-5523-00
BD Cytofix	BD Biosciences	Cat# 554655
BD PermWash	BD Biosciences	Cat# 554723
DNeasy Blood and Tissue Kit	QIAGEN	69504
Genomic DNA Clean & Concentrator Kit	Zymo Research	D4010
RNeasy Mini Kit	QIAGEN	74104
Amaxa Mouse T Cell Nucleofector Kit	Lonza	VPA-1006
Dual Luciferase Assay	Promega	E1910
Deposited Data		
RNA-sequencing of murine WT and MAZR-cKO FOXP3+ regulatory	Gene Expression Omnibus (GEO)	GSE123149
Experimental Models: Cell Lines		
Phoenix-ECO	Nolan Lab, Stanford University	N/A
Experimental Models: Organisms/Strains		
C57BL/6	Jackson Laboratory	N/A
Mouse: MAZRf/f: Patz1$^{tm1.2Welm}$	Abramova et al., 2013; Sakaguchi et al., 2015	MGI: 5572819
Mouse: Cd4-Cre: Tg(Cd4-cre)1Cwi	Chris Wilson (University of Washington, Seattle, USA); Lee et al., 2001	MGI: 2386448
Mouse: Lck-Cre: Tg(Lck-cre)1Cwi	Chris Wilson (University of Washington, Seattle, USA); Lee et al., 2001	MGI: 2448686
Mouse: Tg(Foxp3-DTR/EGFP)23.2Spar	Lahl et al., 2007	MGI: 3849080
Mouse: ThPOK-GFP (Zbtb7b^{tm1Tani})	Ichiro Taniuchi (RIKEN Center for Integrative Medical Sciences, Yokohama, Japan); Setoguchi et al., 2008	MGI: 3774002
Mouse: Rag2$^{-/-}$ (B6.129S(Cg)-Rag2^{tm1Fwa}/FwaOrl)	European Mouse Mutant Archive (EMMA); Taconic	EM: 00162; Taconic: RAGN12; MGI: 1858556

(*Continued on next page*)

Continued		
REAGENT or RESOURCE	SOURCE	IDENTIFIER
Mouse: CD45.1 (B6Rcc.Cg-Ptprc^{a}/Cnrm)	European Mouse Mutant Archive (EMMA); Jackson Laboratories	EM: 01998
Oligonucleotides		
Mazr-fwd	Sigma Aldrich	5′-TGTGTGGTCTGCGGTTCAAG-3′
Mazr-rev	Sigma Aldrich	5′-GAGCATTTCTGGCCTTCTCG-3′
Foxp3-fwd	Sigma Aldrich	5′-GAAAGACAGCAACCTTTTGG-3′
Foxp3-rev	Sigma Aldrich	5′-ACTGCACCACTTCTCTCTGG-3′
Hprt1-fwd	Sigma Aldrich	5′-GCTGGTGAAAAGGACCTCT-3′
Hprt1-rev	Sigma Aldrich	5′-CACAGGACTAGAACACCTGC-3′
Mazr floxed-R6 (genotyping)	Sigma Aldrich	5′-CAACCGGCATAAGCTTTCCC-3′
MAZR floxed-R2 (genotyping)	Sigma Aldrich	5′-GTTATGTTCTATTAAGGTCCAGTGACC-3′
Dereg GFP-fwd (genotyping)	Sigma Aldrich	5′-GCGAGGGCGATGCCACCTACGGCA-3′
Dereg GFP-rev (genotyping)	Sigma Aldrich	5′-GGGTGTTCTGCTGGTAGTGGTCGG-3′
Cd4cre-fwd (genotyping)	Sigma Aldrich	5′-TCTCTGTGGCTGGCAGTTTCTCCA-3′
Cd4cre-rev (genotyping)	Sigma Aldrich	5′-TCAAGGCCAGACTAGGCTGCCTAT-3′
Lckcre-fwd (genotyping)	Sigma Aldrich	5′-GAGTTGTAATGAAGAGGGACAGGT-3′
Lckcre-rev (genotyping)	Sigma Aldrich	5′-CTGAACATGTCCATCAGGTTCTT-3′
Recombinant DNA		
pMIGR1-GFP	Gary Nolan (Stanford University, Stanford, USA)	Addgen 27490
pMIGR1-MAZR-GFP	Bilic et al., 2006	N/A
pGL4-Foxp3pro-luc2	Polansky et al., 2010	N/A
pGL4-CNS1-luc2	Zheng et al., 2010; Schuster et al., 2012	N/A
pGL4-CNS2-luc2	Polansky et al., 2010	N/A
pGL4-CNS3-luc2	Zheng et al., 2010; Schuster et al., 2012	N/A
pGL4-hRLuc (Renilla)	Promega	E2231
Software and Algorithms		
Data analysis: FlowJo v10	FlowJo LLC	N/A
Data analysis: Prism 5.0	GraphPad	N/A
Other		
Annexin V-eFluor450	eBioscience	Cat# 48-8006-74
7-AAD	eBioscience	Cat# 00-6993-50
Cell Proliferation Dye eFluor450	eBioscience	Cat# 65-0842-90
Fixable Viability Dye eFluor	eBioscience	Cat# 65-0866-18

LEAD CONTACT AND MATERIALS AVAILABILITY

Further information and requests for resources and reagents should be directed to and will be fulfilled by the Lead Contact, Wilfried Ellmeier (wilfried.ellmeier@meduniwien.ac.at). This study did not generate new unique reagents.

EXPERIMENTAL MODEL AND SUBJECT DETAILS

Human samples

The Ethics Committee of Hospital District of Southwest Finland approved usage of the blood of unknown donors.

Mice

In this study, *Mazr*$^{F/F}$ mice with a T cell-specific deletion of MAZR (*Cd4*-Cre;*Lck*-Cre; floxed exon 1 of MAZR) (Abramova et al., 2013; Lahl et al., 2007; Sakaguchi et al., 2015) and DEREG *Foxp3*-eGFP reporter BAC transgenic mice, in which GFP expression is driven

by *Fopx3* regulatory elements (Abramova et al., 2013; Lahl et al., 2007; Sakaguchi et al., 2015), were used. *Cd4*-Cre and *Lck*-Cre mice (Lee et al., 2001) were kindly provided by Dr. Chris Wilson. ThPOK-GFP knockin mice (Setoguchi et al., 2008) were kindly provided by Dr. Ichiro Taniuchi. Male and female mice were used at 8-12 weeks of age unless otherwise stated. Animal experiments were evaluated by the ethics committees of the Medical University of Vienna and approved by the Austrian authorities *(GZ:BMWF-66.009/0103-WF/II/3b/2014 and GZ:BMWF-66.009/0105-WF/II/3b/2014).* Mice were bred and maintained in the preclinical research facility of the Medical University of Vienna. Animal husbandry and experimentation were performed in compliance with national laws and according to FELASA and ARRIVE guidelines.

METHOD DETAILS

Genotyping of mice

Primers for genotyping are listed in the STAR Methods. The PCR for the WT (PCR fragment length: 300 bp) and "floxed" *Mazr* (400 bp) allele was carried out for 5 min at 96°C, followed by 39 cycles of 30 s at 94°C, 30 s at 56°C, and 1 min at 72°C. The PCR for the DEREG (GFP) transgene (450 bp) was carried out for 1 min at 96°C, followed by 35 cycles of 1 min at 94°C, 1 min at 60°C, and 1 min at 72°C. The PCR for the *Cd4*-Cre transgene (300 bp) and for the *Lck*-Cre transgene (400 bp) was carried out for 5 min at 96°C, followed by 39 cycles of 30 s at 94°C, 30 s at 56°C, and 1 min at 72°C.

T cell isolation, T cell stimulation, iT_{reg} cultures and intracellular staining

$CD4^+$ T cells were isolated as described (Boucheron et al., 2014). FACS-purified $CD4^+CD44^-CD62L^{hi}$ T cells (0.6×10^6 cells/well) were stimulated (day 0) with plate-bound anti-CD3ε (1 μg/ml; BD Biosciences) and anti-CD28 (3 μg/ml; BD Biosciences) and cultured in 1 mL T cell medium/well (RPMI1640 supplemented with 10% FCS, antibiotics, 50 mM β-ME) in the presence of TGF-β (1 ng/ml; R&D Systems). For proliferation tracking, cells were labeled before culture with cell proliferation dye in eFluor450 (eBioscience) for 10 min at 37°C. For cytokine staining, activated cells (day 3) were restimulated for 4 h with phorbol 12-myristate 13-acetate (PMA; 25 ng/ml; Sigma) and ionomycin (Iono; 750 ng/ml; Sigma) in the presence of GolgiStop (BD Biosciences). For intracellular staining, cells (day 3) were stained with appropriate surface antibodies and fixable viability dye (eBioscience), fixed and permeabilized (eBioscience Foxp3 Staining Buffer Set; BD Cytofix/Cytoperm) and stained with intracellular antibodies.

Flow cytometry and antibodies

Antibodies and dyes used in this study are listed in the STAR methods. Data were collected with a FACS Fortessa or LSR II (BD Biosciences) and analyzed with FlowJo v10 software (TreeStar).

Retroviral infection of $CD4^+$ T_{reg} cells

Preparation of high-titer virus supernatant and retroviral infection was performed as described (Boucheron et al., 2014). Purified $CD4^+CD44^-CD62L^{hi}$ T cells were stimulated (day 0) with plate-bound anti-CD3ε (1 μg/ml; BD Biosciences) and anti-CD28 (3 μg/ml; BD Biosciences) on 48-well plates (0.8×10^6 cells/well) in the presence of TGF-β (1 ng/ml; R&D Systems). One day after anti-CD3ε/anti-CD28 stimulation, $CD4^+$ T cells were suspended in 1 mL viral supernatant containing 10 mg polybrene (H9268; Sigma) and centrifuged at 6000 g for 2 h at 32°C. After spin infection, cells were placed into same 1 mL T cell medium containing 1 ng/ml TGF-β. Cultured cells were analyzed by flow cytometry on day 4.

Generation of bone marrow (BM) reconstituted mice

BM cells were retrovirally infected as described previously (Bilic et al., 2006). For competitive BM transplantation, BM cells from either WT^{Lck} or MAZR-cKO^{Lck} mice (both $CD45.2^+$) were mixed at a ratio of 1:1 with $CD45.1^+$ WT BM cells, and 8×10^6 cells were injected into the tail veins of lethally irradiated $CD45.1^+$ congenic mice. 6-8 weeks after transplantation, reconstituted mice were killed and their cells were analyzed by flow cytometry.

tT_{reg} differentiation cultures

$TCR\beta^+CD4^+CD25^+eGFP^-$ thymocytes were isolated from WT,DEREG and MAZR-cKO,DEREG mice (6-8 weeks) and cultured in a V-bottom 96-well plate (20.000 cells/well) in T cell medium supplemented with 100 U/ml rhIL-2 (PeproTech). After 24 h, cells were harvested and stained with viability dye (eBioscience) and appropriate antibodies and subjected to flow cytometric analysis.

Suppression assays

FACS-purified $CD45.1^+$ $CD4^+CD44^-CD62L^{hi}$ cells were labeled with 20 μM cell proliferation dye eFluor450 (eBioscience) for 10 min at 37°C before culture and activated in the presence of 1×10^5 antigen-presenting cells (irradiated $CD45.2^+$ splenocytes) and 1 μg/ml anti-CD3ε (BD Biosciences). 5×10^4 responder T cells were cultured in U-bottom 96-well plates in T cell medium (supplemented with 1 mM sodium pyruvate and 100 mM non-essential amino acids) at different ratios with FACS-purified $CD45.2^+$ $eGFP^+$ T_{reg} cells isolated from the spleen and lymph nodes of $Mazr^{F/F}$ DEREG *Cd4*-Cre mice. After 72 hours, cells were harvested and stained with appropriate antibodies and subjected to flow cytometric analysis.

Bisulphite sequencing

Genomic DNA from FACS-sorted thymic $CD25^+eGFP^-$ CD4SP precursor T_{reg} cells and $eGFP^+$ T_{reg} cells (isolated from male WT,DEREG and MAZR-cKO,DEREG mice; 6-8 weeks old) was isolated using the DNeasy Blood and Tissue Kit (69504, QIAGEN) and subsequently treated with the Genomic DNA Clean & Concentrator Kit (D4010, Zymo Research), following the suppliers' instructions. The methylation status of the TSDR was analyzed by bisulphite sequencing on genomic DNA as described (Floess et al., 2007).

Immunoblot analysis

For immunoblots with human cells, anti-PATZ1 from Santa Cruz (D-5; sc-390577), anti-human FOXP3 (PCH101; eBioscience) and anti-GAPDH (6C5; HyTest) were used. Mouse TrueBlot (18-8817-33; Rockland Immunochemicals) was used as a secondary antibody.

Synthesis of cDNA and qRTPCR

Total RNA was isolated with RNeasy Mini Kit (QIAGEN). RNA samples were treated with DNase I (Fermentas) and converted into cDNA by SuperScript III reverse transcriptase with random hexamer and oligo(dT) primers according to the manufacturer's protocol (Invitrogen). The iTag Universal SYBR Green System (172-5121; BioRad) were used for quantitative real-time PCR. Primers are listed in the STAR methods. The PCR was carried out for 5 min at 96°C, followed by 39 cycles of 30 s at 94°C, 30 s at 56°C, and 1 min at 72°C.

In vitro luciferase reporter assays

Primary MACS-purified splenic $CD4^+$ T cells were stimulated with plate-bound anti-CD3 (1 μg/ml) and anti-CD28 (3 μg/ml) on a 24-well plate (2×10^6 cells/well) in the presence of TGFβ (1 ng/ml) for 72 hours, and subsequently electroporated with 1 μg Renilla and 6 μg of the indicated pGL4-based luciferase constructs using the Amaxa Mouse T cell Nucleofector Kit (Lonza). *Foxp3* promoter, CNS1-*Foxp3* promoter, CNS2-*Foxp3* promoter and CNS3-*Foxp3* promoter constructs were previously described (Polansky et al., 2010; Schuster et al., 2012). After transfection, the cells were seeded on an anti-CD3/anti-CD28-coated 24 well plate for 42 hours. Luciferase activity was measured using the dual luciferase assay system (Promega) on a Mithras LB 940 (Berthold Technologies).

DSS-induced colitis and T cell isolation from small intestine

Mice were administered 3% DSS in drinking water over 9 days, followed by 1.5% DSS for another 3 days, while body weight was monitored regularly. On day 12, mice were sacrificed, colon length measured and swiss rolls were prepared according to published protocol (Moolenbeek and Ruitenberg, 1981) and fixed overnight in 4% para-formaldehyde (PFA) for subsequent H&E staining. Disease score was assessed by 5 independent researchers in a double-blinded fashion according to a pre-determined scoring scheme considering crypt damage and inflammatory cell infiltration, epithelial ulceration and goblet cell depletion (divided into distal, middle, proximal colon with a severity score of each 0-3 points, giving a total maximum of 9 possible points for the highest disease severity). T cells were isolated from spleens, mesenteric LN and small intestines of diseased mice, stained with appropriate antibodies and subjected to flow cytometric analysis. For T cell isolation from small intestine, Peyer's batches and mucus were removed, tissue cut into small pieces and incubated with 5 mM EDTA solution to receive the intraepithelial lymphocytes (IEL). Subsequently, remaining tissue was digested with 100 U/ml collagenase Type II (GIBCO) for 1 hour, followed by a Percoll (Sigma) gradient centrifugation to receive lymphocytes from the lamina propria (LPL).

Adoptive T cell transfer colitis

4×10^5 FACS-purified naive $CD45RB^{hi}$ $CD4^+$ T cells from $CD45.1^+$ congenic mice were injected i.p. into *Rag2*$^{-/-}$ mice together with 1×10^5 $CD45.2^+$ T_{reg} cells, either from *Mazr*$^{F/F}$ DEREG (WT) or *Mazr*$^{F/F}$ DEREG *Cd4*-Cre (cKO) mice. Mice were monitored for 8 weeks and subsequently sacrificed for organ analysis. For histological analysis, swiss rolls were prepared from coli of diseased mice as described (Moolenbeek and Ruitenberg, 1981). Disease severity was scored as described above. Lamina propria lymphocytes (LPL) and intraepithelial lymphocytes (IEL) were isolated from small intestines as described above and analyzed by flow cytometry.

Homeostatic T cell expansion upon adoptive transfer

2×10^6 FACS-purified naive ($CD44^-CD62L^{hi}$) $CD4^+$ T cells from $CD45.1^+$ congenic mice were i.v.-injected into *Rag2*$^{-/-}$ mice together with either 5×10^5 $CD45.2^+$ WT,DEREG or MAZR-cKO,DEREG T_{reg} cells. After 7 days, mice were sacrificed for organ analysis.

RNA-Sequencing and sample preparation

Total RNA was prepared from approximately 0.8 - 2×10^6 FACS-purified WT,DEREG and MAZR-cKO,DEREG naive ($CD44^-CD62L^{hi}$) $CD4^+$ T cells and $CD4^+eGFP^+$ T_{reg} cells with the RNeasy Mini Kit (QIAGEN). RNA-seq libraries were prepared using a Sciclone NGS Workstation (PerkinElmer) and a Zepyhr NGS Workstation (PerkinElmer) with the TruSeq Stranded mRNA LT sample preparation kit (Illumina). RNA and library concentrations were determined using Qbit 2.0 Fluorometric Quantitation (Life Technologies), while RNA and library integrities were determined using Experion Automated Electrophoresis System (Bio-Rad). The libraries were sequenced by the Biomedical Sequencing Facility at CeMM using the Illumina HiSeq 3000/4000 platform and the 50-bp single-read configuration.

Human CD4$^+$ T cell isolation and differentiation into iT$_{reg}$ cells

CD4$^+$ T cells were isolated from human umbilical cord blood as described (Hawkins et al., 2013). iT$_{reg}$ and control Th0 cells were differentiated as previously described (Ullah et al., 2018) and used for Western Blot analysis. Briefly, CD25$^+$ cells were depleted using LD columns and a CD25 depletion kit (Miltenyi Biotec). 2 × 10^6 cells/mL CD4$^+$CD25$^-$ cells from three or more donors were activated directly or pooled before activation with plate-bound anti-CD3 (500 ng/24-well culture plate well; Immunotech) and soluble anti-CD28 (500 ng/mL; Immunotech) in X-vivo 15 serum-free medium (Lonza). For iT$_{reg}$ differentiation, the medium was supplemented with IL-2 (12 ng/mL), TGFβ (10 ng/mL) (both from R&D Systems), all-trans retinoic acid (10 nM; Sigma-Aldrich), and human serum (10%) and cultured at 37°C in 5% CO_2. Control Th0 cells were stimulated with plate-bound anti-CD3 and soluble anti-CD28 in X-vivo 15 serum-free medium without cytokines.

QUANTIFICATION AND STATISTICAL ANALYSIS

Bioinformatic analysis of RNA-sequencing data

The quality of the sequenced reads was checked using FastQC tool (Andrews, 2010). STAR 2.5.2b (Dobin et al., 2013) was used to align the reads to the mouse reference genome mm10 (UCSC; downloaded from Illumina iGenomes website). The number of uniquely mapped reads associated with each gene according to Ensembl gene annotation was counted using subread v1.5.1 package (Liao et al., 2014). The downstream data analysis was performed using R version 3.4 (R Team, 2015) and its corresponding Bioconductor module (Gentleman et al., 2004). The count data were normalized for library size using the Trimmed Mean of M-values (TMM) method implemented in edgeR R package (Robinson et al., 2010). Genes that did not have at least one count per million (CPM) in at least three samples among the compared sample groups were filtered out as lowly expressed. Prior to statistical testing, an offset of 1 was added to the normalized expression values and the data were log2 transformed. R package ROTS (Suomi et al., 2017) was used for performing the statistical testing and p value < 0.05 and absolute fold change > 1.5 were required for detecting the differentially expressed genes. The *Gh* gene was removed from the final DE gene list as the inspection of the aligned reads revealed that the alignments for *Gh* had almost identical positions on a narrow region and contained many mismatches.

Statistical analysis

No statistical methods were used to predetermine the sample size. All statistical analyses were performed using Prism Software (GraphPad Inc). P values were calculated with an unpaired two-tailed Student's t test (a normal distribution of data points was assumed; variances were assessed and if necessary, an unpaired t test with Welch's correction was applied). No data were excluded. For disease scoring, sample IDs were blinded. Data shown indicate the mean unless otherwise stated.

DATA AND CODE AVAILABILITY

The RNA-seq data have been deposited in the GEO database under ID code GSE123149.